Mycobacterium trehalose polyphleates are required for mycobacteriophage infection

Running title: Phage requirement for trehalose polyphleates

Katherine S. Wetzel[1#], Morgane Illouz[2#], Lawrence Abad[1], Haley G. Aull[1], Daniel A. Russell[1], Rebecca A. Garlena[1], Madison Cristinziano[1], Silke Malmsheimer[2], Christian Chalut[3], Graham F. Hatfull[1]*, and Laurent Kremer[2,4]*

[1]Department of Biological Sciences University of Pittsburgh, Pittsburgh, PA 15260 USA

[2]Centre National de la Recherche Scientifique UMR 9004, Institut de Recherche en Infectiologie de Montpellier (IRIM), Université de Montpellier, 1919 route de Mende, 34293, Montpellier, France.

[3]Institut de Pharmacologie et de Biologie Structurale, Université de Toulouse, CNRS, UPS, Toulouse, France

[4]INSERM, IRIM, Montpellier, France

[#]Authors contributed equally

Corresponding authors: gfh@pitt.edu; laurent.kremer@irim.cnrs.fr

Abstract

Mycobacteriophages are good model systems for understanding their bacterial hosts and show promise as therapeutic agents for nontuberculous mycobacterium infections. However, little is known about phage recognition of *Mycobacterium* cell surfaces, or what molecules act as phage receptors. We show here that surface-exposed trehalose polyphleates (TPPs) are required for infection of *Mycobacterium abscessus* and *Mycobacterium smegmatis* by clinically useful phages BPs and Muddy, and that TPP loss leads to defects in adsorption, infection, and confers resistance. Transposon mutagenesis indicates that TPP loss is the sole mechanism for phage resistance. However, both phages can overcome TPP loss through single amino acid substitutions in their tail spike proteins, suggesting that TPPs act to facilitate receptor recognition. Some *M. abscessus* clinical isolates have defects in TPP synthesis but the phage tail spike mutants could effectively substitute for their parent phages in clinical use to circumvent resistance due to TPP loss.

52 **Introduction**

53

54 Nontuberculous mycobacteria (NTM) include several important human pathogens such as
55 *Mycobacterium abscessus* and *Mycobacterium avium* [1,2]. These infections are often refractory
56 to effective antibiotic treatment due to both intrinsic and acquired resistance mutations, and new
57 treatment options are needed [3]. The therapeutic application of mycobacteriophages shows
58 some promise for the treatment of pulmonary infections in cystic fibrosis patients [4-6],
59 disseminated infection following bilateral lung transplantation [4], and disseminated
60 *Mycobacterium chelonae* infection [7]. However, broadening therapy beyond single-patient
61 compassionate use applications will require expansion of the repertoire of therapeutically useful
62 phages, and increasing host range such that a higher proportion of clinical isolates can be
63 treated [5,8,9]. Clinical administration of bacteriophages is anticipated to give rise to phage
64 resistant mutants and disease recurrence [10], but the frequency and mechanisms of
65 mycobacteriophage resistance are poorly understood [11]. Very few mycobacteriophage receptors
66 are known, although glycopeptidolipids (GPLs) are proposed as receptors for
67 mycobacteriophage I3 in *Mycobacterium smegmatis* [12].

68

69 Over 12,000 individual mycobacteriophages have been described, with most being isolated on
70 *M. smegmatis* [13]. The genome sequences of 2,200 of these show them to be highly diverse
71 genetically and pervasively mosaic [14,15]. They can be sorted into groups of genomically related
72 phages (e.g. Cluster A, B, C etc.), some of which can be readily divided into subclusters (e.g.
73 Subcluster A1, A2, A3 etc.) based on sequence variation [16,17]. Seven of the sequenced phages
74 currently have no close relatives and are designated as 'Singletons'. A subset of these phages
75 has relatively broad host range and are also able to efficiently infect *Mycobacterium*
76 *tuberculosis*, including phages in Clusters/Subclusters A2, A3, G1, K1, K2, K3, K4, and AB [18,19].
77 A similar subset of phages also infect some clinical isolates of *M. abscessus*, although it is

78 noteworthy that phage host ranges on these strains is highly variable (even for related phages
79 within clusters/subclusters), and is highly variable among different clinical isolates [4,9]. There is
80 also substantial variation in the outcomes of phage infection of *M. abscessus* strains, with
81 notable differences between rough and smooth colony morphotypes [9]. For example, a smaller
82 proportion of smooth isolates are susceptible to phage infection than rough strains – as
83 determined by plaque formation – and none of the smooth strains are efficiently killed by any
84 phage tested [9].
85
86 Mycobacterial cell walls characteristically have a mycolic acid-rich outer layer referred to as the
87 mycobacterial outer membrane or mycomembrane [20]. In addition to abundant mycolic acids,
88 there are numerous other types of complex molecules including multiple acylated lipids such as
89 di- and polyacyltrehalose (DAT and PAT), phthiocerol dimycocerosate (PDIM) and
90 sulfoglycolipids (SGL), although not all are found in all *Mycobacterium* species. Smooth strains
91 of *M. abscessus* have abundant GPLs although these are lacking or greatly less abundant in
92 rough strains [21,22]. Recently, it has been shown that some mycobacterial species, including *M.*
93 *abscessus*, have trehalose polyphleates (TPPs), which are high-molecular-weight, surface-
94 exposed glycolipids, in their cell walls [23,24]. These TPPs may be important for *M. abscessus*
95 virulence and are associated with clumping and cording [24]. A five gene cluster, – including a
96 polyketide synthetase (Pks) – is required for TPP biosynthesis and TPP precursor (DAT)
97 transport to the outer surface of the cell by MmpL10 [25]. TPPs are not present in *M. tuberculosis*
98 although DAT and PAT are [25]. The specific roles of TPPs are not known, but their position on
99 the outer surface makes them candidates for use as phage receptors.
100
101 Here, we show that TPPs are required for the binding and infection of *M. abscessus* by phages
102 BPs and Muddy. These phages share little or no nucleotide similarity but both have been used
103 therapeutically, sometimes in combination with each other [4,26]. *M. abscessus* transposon

104 insertion mutants that are resistant to these phages map in four of the five genes involved in
105 TPP synthesis, but are also located in at least 11 other genetic loci, all of which cause loss of
106 TPP. Spontaneous phage resistant mutants of some *M. abscessus* clinical isolates also have
107 mutations in the known TPP synthesis genes. The requirement of TPP for efficient phage
108 binding can be readily overcome by mutations in phage tail spike proteins. Thus, although TPP
109 is required for phage infection it likely acts to facilitate recognition of an unknown receptor by the
110 phages, and the phage mutants enable a bypass for the TPP requirement. Resistance from
111 TPP loss may play an important role in how these phages are used therapeutically.
112
113 **Results**
114
115 **Development of a transposon system for mutagenesis of *M. abscessus* clinical isolates**
116
117 Although there are numerous *M. abscessus* isolates available in which we could potentially
118 construct mutant libraires, many are not sensitive to phage infection. We chose *M. abscessus*
119 GD01 (subspecies *massiliense*) as it was the first clinical isolate treated therapeutically and is
120 sensitive to and killed well by phages Muddy, ZoeJ∆*45*, and BPs∆*33*HTH_HRM10 [the initial
121 therapeutic cocktail [4]]. These phages are genomically distinct, mapping in Clusters AB, K2, and
122 G1, respectively. ZoeJ∆*45* is a lytic derivative of its parent ZoeJ [27], and BPs∆*33*HTH_HRM10 is
123 a lytic derivative of BPs [28], carrying a mutation in the portal gene that facilitates efficient infection
124 of GD01 [4]; Muddy is a lytic phage that efficiently infects GD01 [4].
125
126 Strain GD01 has a rough colony morphotype and is also susceptible to phages Itos and
127 Faith1∆*38-40* (both in Subcluster L2) and Isca (Subcluster A3). Extant mycobacteria transposon
128 mutagenesis systems typically use a kanamycin resistance Kan^R-marked transposon

129 (MycoMarT7 transposon) carried on a temperature-sensitive derivative of phage TM4 [29] (Fig.
130 1A). However, strain GD01 (and many other *M. abscessus* clinical isolates) is resistant to
131 kanamycin (MIC>128 µg/mL) [30], and engineering of the transposon was required to include an
132 alternative selectable genetic marker. Screening of strain GD01 against different antibiotics
133 revealed sensitivity to hygromycin at high concentrations (1 mg/mL) in solid media.
134
135 We used a phage engineering strategy (CRISPY-BRED) [31] to replace the KanR marker in the
136 MycoMarT7 transposon with a hygromycin-resistance (HygR) marker (Fig. 1A). We constructed
137 two transposon variants, one that included the R6Kγ origin of replication (present in the
138 MycoMarT7 transposon) and one without it. The shorter transposon (named MycoMarT7-Hyg2
139 transposon) transduced strain GD01 ~100 times more efficiently than the longer MycoMarT7-
140 Hyg transposon; this difference in efficiency was not observed for *M. smegmatis* (data not
141 shown). We transduced strain GD01 with MycoMarT7-Hyg2 and selected Hyg-resistant
142 transductants on solid media to yield a random mutagenesis library of clones (Fig. 1B). We note
143 that phage TM4 – the parent of these transposon delivery phages – does not form plaques on
144 lawns of *M. abscessus* GD01 or other *M. abscessus* strains [9] but efficiently delivers DNA to *M.*
145 *abscessus* cells [32].
146
147 **Transposon insertion mutants resistant to phages BPsΔ*33*HTH_HRM10 and Muddy**
148
149 Phage challenges of bacterial transposon insertion mutagenesis libraries are powerful
150 approaches to identify host factors required for phage infection and phage receptors [33-36]. To
151 identify phage resistant mutants of *M. abscessus*, the GD01 Tn library was plated on solid
152 media seeded with 10^9 plaque forming units (pfu) of either phage BPsΔ*33*HTH_HRM10 or
153 phage Muddy. Survivors grew as single colonies at a frequency of ~10^{-3} of viable cells on both

154 phage-seeded plates. Individual colonies were picked, rescreened, and analyzed by a targeted
155 PCR strategy to determine the transposon insertion site. The sites of transposon insertion could
156 be identified for 17 of the BPs∆*33*HTH_HRM10 resistant colonies and 11 of the Muddy resistant
157 colonies; 26 of the insertions were unique (Table 1). Interestingly, seven of the 26 unique
158 BPs∆*33*HTH_HRM10-resistant mutants map in the TPP synthesis genes (Table 1, Fig. 1C, D),
159 but eight of the nine unique Muddy-resistant mutants also map in these genes, suggesting that
160 normal TPP synthesis is required for infection of both BPs∆*33*HTH_HRM10 and Muddy (Fig.
161 1C, D, Table 1). Eight of the unique transposon insertions are in the *fadD23* gene (the 3'-most
162 gene in the leftwards-transcribed four-gene operon; Fig. 1C) and a single insertion is in *mmpL10*
163 (Fig. 1C); transposon insertions in *papA3*, *mmpL10* and *pE* may be genetically polar and also
164 affect *fadD23* expression. Curiously, no insertions were recovered in the *pks* gene, despite it
165 being a much larger target (11 kbp) than the other four genes and is reported elsewhere as
166 being non-essential [37]. The other 11 mutants map in 11 separate genetic loci that are generally
167 not closely linked to the TPP synthesis genes (Table 1).
168
169 To confirm phage resistance, lysates of phages BPs∆*33*HTH_HRM10 and Muddy were tenfold
170 serially diluted and spotted onto lawns of transposon insertion TPP mutant strains on solid
171 media (Fig. 1E). When tested on a *fadD23* mutant, the efficiency of plaquing (EOP) of
172 BPs∆*33*HTH_HRM10 was reduced by seven orders of magnitude, although some individual
173 plaques were observed at the highest concentration of phage, possibly representing derivatives
174 escaping the mutational defect. When Muddy was plated on the same strain, the (EOP) was not
175 substantially reduced, but the plaques (and spots) were much more turbid than on the parental
176 GD01 strain (Fig. 1E). Similarly to BPs∆*33*HTH_HRM10, within higher concentration spots clear
177 plaques were observed possibly representing derivatives that escape the resistance. These
178 general patterns of infection for BPs∆*33*HTH_HRM10 and Muddy were the same for all of the

179 TPP pathway mutants tested, regardless of whether they were isolated as being resistant to
180 Muddy or BPs∆*33*HTH_HRM10. We also tested whether the TPP pathway mutants are co-
181 resistant to the other phages that GD01 is sensitive to (ZoeJ∆*43-45*, Itos, and Faith1∆*38-40*)
182 (Fig. 1E). All three infect all of the mutants tested similarly to the parental GD01 strain, and thus
183 the phage resistant phenotype is specific to Muddy and BPs∆*33*HTH_HRM10 among those
184 tested here (Fig. 1E).
185
186 To confirm that phage resistance is a direct consequence of the transposon insertions, we
187 constructed a plasmid carrying *fadD23* under an inducible promoter in an integration vector. The
188 *fadD23* plasmid was successfully transformed into GD01Tn_BPsHRM10_RM1, harboring a Tn
189 insertion in *fadD23* (Table 1) and transformants were tested for phage sensitivity. When grown
190 in the presence of anhydrotetracycline (ATc) inducer, expression of FadD23 complements the
191 *fadD23*::Tn insertion and restores the wild-type patterns of infection of both
192 BPs∆*33*HTH_HRM10 and Muddy (Fig. 1F). Plasmids carrying *papA3* or *fadD23*, *pE*, *mmpL10*
193 and *papA3* under control of the native promoter did not efficiently transform strain GD01 and
194 thus complementation could not be readily tested.
195
196 **GD01 mutants resistant to BPs∆*33*HTH_HRM10 and Muddy all show loss of TPP**
197
198 To test whether the TPP pathway mutants are defective in synthesis and assembly, cell wall
199 lipids were extracted from four representative mutants (in *pE*, *mmpL10*, *fadD23* and *papA3*) and
200 analyzed by thin layer chromatography (TLC) (Fig. 2A); all four showed complete loss of TPP.
201 Previously it was reported that interruption of TPP precursor transport (as in an *mmpL10*
202 mutant), or loss of PE which is needed for the final step of TPP synthesis (see Fig. 1D), results
203 in accumulation of the DAT precursor [23,25]. Here, we observe DAT accumulation in the *mmpL10*

204 transposon insertion mutant, but not in the *pE* mutant (Fig. 2A); it plausible that the *pE*
205 transposon insertion is genetically polar and leads to loss of fadD23 expression, and a failure to
206 synthesize DAT. We also examined the 11 additional mutants with mutations in non-TPP
207 pathway genes. All of these have lost TPP and one appears to accumulate DAT (*MAB_3426c*;
208 Fig. 2B). It is unlikely that any of the mutants also carry spontaneous mutations in the TPP
209 synthesis pathway genes, as the transposon insertion mutants were recovered at a ~10^3-fold
210 higher frequency than spontaneous phage resistant mutants (Fig. 1B).
211
212 The finding that all of the BPs- and Muddy-resistant mutants have lost TPP is unexpected, as it
213 suggests that the remaining 11 genes are involved, directly or indirectly, with some aspect of
214 TPP synthesis, regulation, assembly, or transport. We tested these mutants for their phage
215 infection profiles and showed that all have very similar phenotypes to the TPP pathway mutants,
216 with lack of plaque formation by BPs∆*33*HTH_HRM10, reduced EOP of Muddy infection, and
217 sensitivity to ZoeJ∆*43-45* (Fig. 2C, S1).
218
219 **BPs∆*33*HTH_HRM10 mutants in the predicted tail spike gene escape the TPP requirement**
220
221 Although BPs_∆*33*HTH_HRM10 does not form plaques well on *M. abscessus* strains mutated in
222 the TPP synthesis pathway, clear plaques were observed at high phage titers, and are
223 candidates for derivatives escaping TPP loss (Fig. 1E). Five individual plaques were purified,
224 shown to have heritable infection of TPP mutants, and were further characterized. Two were
225 isolated on *M. abscessus* GD01 *fadD23::Tn* (phKSW2 and phKSW3), two were isolated on
226 GD01 *pE::Tn* (phKSW4 and phKSW5), and one was isolated on GD180_RM2 (see below)
227 (BPs_REM1) (Table 2). Sequencing showed that all have substitutions in gp22, the predicted
228 BPs tail spike, and that phKSW2 and pKSW4 carry the same substitution (L462R) (Table 2).

229 The mutants are able to form clear plaques on all TPP synthesis pathway mutants tested (Fig.
230 3A). Interestingly, two of these substitutions, gp22 A306V and A604E, were reported previously
231 as BPs host range mutants able to infect *M. tuberculosis* [18,28]. The gp22 A604E substitution is
232 also present in phage BPs∆*33*HTH_HRM^{GD03} that infects some other *M. abscessus* strains [4].
233 Although phKSW2 and phKSW4 have a gp22 L462R substitution, BPs_REM1 has both a gp22
234 L462R substitution and a G780R substitution. BPs_REM1 forms somewhat clearer plaques than
235 phKSW4 on the TPP mutants (Fig. 3A) suggesting the G780R has an additive effect towards
236 clear plaque formation.
237
238 **TPPs are required for efficient adsorption of BPs∆*33*HTH_HRM10 to *M. abscessus* GD01**
239 Because TPPs are surface-exposed, and are required for BPs∆*33*HTH_HRM10 infection, we
240 tested if they are required for adsorption (Fig. 3B). Wild-type BPs has been reported previously
241 to adsorb rather poorly to wild-type *M. smegmatis* [18] and BPs∆*33*HTH_HRM10 adsorption is
242 similarly poor on *M. abscessus* GD01 (Fig. 3B). However, BPs∆*33*HTH_HRM10 shows a strong
243 defect in adsorption to the GD01 *fadD23*::Tn mutant (Fig. 3B, left panel). Interestingly, the
244 BPs∆*33*HTH_HRM10 gp22 A604E mutant phage (phKSW1) adsorbs considerably faster to
245 GD01 cells than its parent phage (Fig. 3B, middle panel), similar to its improved adsorption to
246 *M. smegmatis* [18]. However, it shows only a small improvement in adsorption relative to its parent
247 phage on the GD01 *fadD23*::Tn mutant (Fig. 3B). In contrast, ZoeJ∆*43-45* adsorbs similarly to
248 both *M. abscessus* strains (Fig. 3B, right panel).
249
250 **Muddy mutants in the predicted tail spike gene *24* also escape the TPP requirement**
251
252 We similarly isolated a resistance escape mutant of phage Muddy (Muddy_REM1, Table 2) from
253 an *M. abscessus* Muddy resistant mutant (*M. abscessus* GD180_RM2, see below) and

254 characterized its infection of TPP pathway mutants (Fig. 3C). We also tested three Muddy
255 derivatives previously reported as having expanded host ranges on *M. tuberculosis*, being able
256 to efficiently infect some clinical isolates that wild-type Muddy does not [19]. We observed efficient
257 infection of all of the TPP pathway mutants by Muddy_REM1 mutant, as well as by
258 Muddy_HRM^{N0052}-1 and Muddy_HRM^{N0157}-1. In contrast, Muddy_HRM^{N0157}-2 gives very turbid
259 plaques on all of the mutants similarly to wild-type Muddy (Fig. 3C). Sequencing showed that
260 Muddy_REM1 contains a single base substitution in the putative tail spike gene *24* conferring a
261 E680K substitution (Table 2). Interestingly, this is the same substitution as in Muddy_HRM^{N0052}-
262 1; Muddy_HRM^{N0157}-1 and Muddy_HRM^{N0157}-2 have G487W and T608A substitutions in gp24,
263 respectively [19]. We note that TPPs are absent from *M. tuberculosis* cell walls [23].
264
265 **Isolation of spontaneous *M. abscessus* phage resistant mutants in the TPP pathway**
266 We previously isolated mutants of *M. abscessus* clinical strains that are resistant to BPs
267 variants *in vitro* by challenging phage–susceptible strains with phages and then recovering
268 survivors [9]. Two of the strains isolated (GD17_RM1 and GD22_RM4, Table 3) have mutations in
269 *pks* (*MAB_0939*) and are at least partially resistant to BPs∆*33*HTH_HRM10 [9]. We have similarly
270 isolated three additional spontaneous mutants resistant to BPs∆*33*HTH_HRM10, two of which
271 (GD38_RM2 and GD59_RM1) have mutations in *pks*; the third (GD180_RM2) has a nonsense
272 mutation in *mmpL10* (Table 3). BPs∆*33*HTH_HRM10 does not form plaques on mutants GD38_
273 RM2, GD17_RM1 or GD59_RM1 and very small plaques at a reduced EOP on GD22_RM4
274 (Fig. 4A). These mutants thus confirm that point mutations in *M. abscessus* TPP synthesis
275 genes can give rise to BPs and Muddy resistance, although these have not been observed
276 clinically [5], suggesting that TPP synthesis may be required for fitness in an ongoing human
277 infection. They also show that Pks is required for BPs and Muddy infection, even though we did

278 not isolate any transposon insertions in *pks*. Similarly to the transposon insertion mutants, these
279 mutants are infected well by other phages we tested (Fig. 4A).
280
281 The *M. abscessus* Pks protein (MAB_0939) is a 3697-residue multidomain protein (Fig. 4B).
282 Two of the spontaneously resistant mutants have frameshift mutations close to the midpoint of
283 the gene (at codons 2,115 and 2,389, Table 3, Fig. 4B) and two others have amino acid
284 substitutions in the N-terminal Keto-synthase (KS) domain (Table 3, Fig. 4B). We note that the
285 two frameshift mutations are in the second Acyltransferase (AT) domain and leave the upstream
286 domains intact (Fig. 4B); it is plausible that the domains C-terminal to the frameshift mutations
287 are not required for viability.
288
289 ***M. abscessus* spontaneous phage resistant mutants are also defective in TPPs**
290
291 Spontaneous mutants GD22_RM4 and GD180_RM2 are defective in *pks* and *mmpL10,*
292 respectively (Fig. 5A), and we showed that both show loss of TPP in their surface lipids (Fig.
293 5B), as anticipated. We successfully complemented both mutants and demonstrated that
294 complementation fully restores BPs∆*33*HTH_HRM10 infection (Fig. 5C) as well as TPP
295 synthesis (Fig. 5B). To further characterize these infections, we tested a reporter phage
296 derivative of BPs expressing mCherry [38], which behaves similarly to BPs∆*33*HTH_HRM10 in
297 plaque assays (Fig. 5B). Both phages efficiently kill the parental GD22 and GD180 strains in
298 liquid culture but are defective in infecting both the GD22_RM4 and GD180_RM2 mutants (Fig.
299 5D); complementation fully restores infection of GD180_RM2, and partially restores infection of
300 GD22_RM4 (Fig. 5D). Microscopic analysis of infection by the mCherry reporter phages showed
301 fluorescence and successful infection of the parental strains, loss of fluorescence in both
302 resistant mutants, and restoration in the complemented strains (Fig. 5E). Quantification shows

303 that the proportion of infected cells in the resistant mutants is less than 1%. (Fig. 5F). These
304 data are consistent with an early defect in phage infection in these resistant mutants,
305 presumably due to loss of adsorption to the cell surface.
306
307 **Distribution of TPP synthesis genes in *M. abscessus* clinical isolates**
308
309 *M. abscessus* clinical isolates vary greatly in their ability to be infected by phages
310 BPs_Δ*33*HTH_HRM10 and Muddy [9], raising the question as to whether variation in TPP content
311 contributes to these infection profiles. Analysis of the amino acid sequences of the TPP
312 synthesis pathway proteins (Pks, PE, PapA3, MmpL10 and FadD23) of 143 sequenced clinical
313 isolates and reference strain ATCC 19977 identified 37 distinct genotypes that generally
314 correlate with global nucleotide similarity (Fig. 6A); however, no evident correlation between
315 these variations and sensitivity to BPs_Δ*33*HTH_HRM10 and/or Muddy was observed (Fig. 6A).
316 Most of the variation observed reflects amino acid substitutions, although two strains (GD262
317 and GD273) have identical large deletions in *pks* (3,645 bp) and two others (GD155 and
318 GD286) have translocations resulting in a 30.2 kbp insertion in *pks* (Fig. 6B). Plaque assays
319 with Muddy showed that GD273 and GD286 behave consistently with TPP loss, and the phage
320 resistance escape mutant Muddy_HRM^{N0052}-1 overcomes the TPP requirement (Fig. 6C).
321 Interestingly, GD262, GD273 and GD286 are not susceptible to BPsΔ*33*HTH_HRM10 nor to its
322 phage resistance escape mutant BPs_REM1 (Fig. 6C), and these strains likely carry additional
323 phage defense mechanisms that target BPs and its derivatives. GD155 has a smooth colony
324 morphotype and is not susceptible to any of the phages tested here.
325
326 ***M. smegmatis* mutants in the TPP synthesis pathway are resistant to phages**
327 **BPs_Δ*33*HTH_HRM10 and Muddy**
328

329 Because *M. smegmatis* is genetically tractable and is susceptible to a very large and diverse set
330 of phages, we also examined the roles of TPPs in that host. Several previously constructed
331 mutants in the TPP synthesis genes and complemented strains were available [23,39] including
332 strains with deletions of *pks (MSMEG_0408)*, *mmpL10 (MSMEG_0410)*, and *pE*
333 *(MSMEG_0412)*. As expected, Δ*pks,* Δ*mmpL10* and Δ*pE* mutants failed to produce TPPs, whilst
334 complementation of all three mutants restores the presence of TPPs and DAT (Fig. 7A). We
335 observed overall similar although milder phenotypes of BPsΔ*33*HTH_HRM10 and Muddy
336 infection as for *M. abscessus* GD01, although BPsΔ*33*HTH_HRM10 forms very turbid plaques
337 on the Δ*pks* and Δ*papA3* mutants but infects Δ*fadD23* similar to wild-type *M. smegmatis* (Fig. 7A
338 and Fig. S2). The efficient infection of the Δ*fadD23* mutant is consistent with previous reports of
339 incomplete TPP loss in such strains, possibly due to an unidentified fatty acyl-AMP ligase
340 partially overcoming this defect [23]. Muddy similarly forms very turbid plaques on the Δ*pks* and
341 Δ*papA3* mutants, but only milder so on the Δ*fadD23* mutant (Fig. 7A). Interestingly, the two
342 BPs_Δ*33*HTH_HRM10-derived host range mutants tested restore normal infection to the *M.*
343 *smegmatis* TPP mutants (Fig. 7A). In addition, all of the Muddy host range mutants restore
344 normal infection of any of the *M. smegmatis* TPP mutants, as reflected in formation of clearer
345 plaques rather than changes in EOP (Fig. 7A). Complementation of the Δ*papA3* mutant with a
346 plasmid (pKSW131) carrying the *M. abscessus* GD01 *fadD23*, *mmpL10*, *pE*, and *papA3* genes
347 successfully restored normal plaque formation by both Muddy and BPsΔ*33*HTH_HRM10 (Fig.
348 S2A), and the Δ*pks*, Δ*mmpL10*, and Δ*pE* mutants were all successfully complemented with the
349 individual corresponding genes (Fig. S2B).
350
351 The *M. smegmatis* Δ*pks*, Δ*mmpL10* and Δ*pE* mutants all have surface lipids from which TPPs
352 are absent (Fig. 7B). In addition, the Δ*pE* mutant accumulates DAT at the bacterial surface (Fig.
353 7B; see Fig. 1D) as reported previously [23]. Complementation of all three mutants restores the

354 presence of TPPs and DAT (Fig. 7B). BPs_Δ*33*HTH_HRM10 and its mCherry derivatives are
355 both defective in liquid infection of all three *M. smegmatis* mutants, and efficient infection and
356 lysis is restored by complementation (Fig. S3A). The mCherry reporter phage shows
357 fluorescence in wild-type *M. smegmatis*, but loss of fluorescence in infection of all three
358 mutants, with restoration of infection in the complemented strains (Fig. S3B). Flow cytometry
359 quantification shows that infection is reduced to less than 1% of the cells in all three mutants,
360 and complementation restores infection efficiency to levels similar to wild-type *M. smegmatis*
361 (Fig. S3C). In addition, the mCherry fluorophage behaves similarly to its parent in plaque assays
362 on *M. smegmatis* mutant and complemented strains (Fig. S2B).
363
364 We tested adsorption of BPsΔ*33*HTH_HRM10 and the phKSW1 resistance escape mutant to
365 wild-type *M. smegmatis* and the Δ*pks* mutant (Fig. 7C). The adsorption kinetics are similar to
366 those seen in *M. abscessus* (Fig. 3B) although we note that the resistance escape mutant
367 phage (phKSW1) has substantially improved adsorption to the Δ*pks* mutant relative to the *M.*
368 *abscessus fadD23* mutant. ZoeJΔ*43-45* shows no adsorption defect to the Δ*pks* mutant (Fig.
369 7C).
370
371 We next explored a panel of additional *M. smegmatis* phages for their infection profiles on the
372 *M. smegmatis* Δ*pks* mutant (Fig. 7D). Most of the phages tested plaque similarly on the Δ*pks*
373 and wild-type strains or with relatively mild EOP reductions, with three notable exceptions:
374 ShedlockHolmes, MsGreen, and Papyrus, in Clusters/Subclusters K3, L3, and R, respectively,
375 that have more pronounced reductions in EOP (Fig. 7D). MsGreen and ShedlockHolmes have
376 tail genes related to Muddy gene *24*, although we note that ZoeJ does so also, and yet is not
377 dependent on TPPs for infection. However, such variation is not unexpected, as the escape

378 mutant observations show that only a single amnio acid substitution is sufficient to confer TPP
379 independence (Figs. 3A, 3C, 7A).
380
381 **Discussion**
382
383 We have shown here that trehalose polyphleates play a key role in phage infection of both *M.*
384 *abscessus* and *M. smegmatis*. TPPs, one of the largest known lipids in mycobacteria, are
385 structurally related to the sulfolipids SL-1 and polyacylated trehalose PAT, which, in contrast to
386 TPPs, are found exclusively in *M. tuberculosis*. While the biosynthetic pathway of TPPs has
387 been discovered recently, their general roles in mycobacterial physiology and/or growth remains
388 unclear. One study has proposed a role of TPPs in the formation of clumps and cording in *M.*
389 *abscessus*, an observation based on the fact that extraction of the cell surface-associated lipid
390 fraction (containing TPPs) by petroleum ether resulted in the loss of corded bacilli [24]. However,
391 as shown in this study, many TPP-defective *M. abscessus* strains (either selected *in vitro* for
392 phage resistance, or naturally in patient isolates) present a rough morphotype – typically
393 associated with cording – indicating that TPP do not play a direct role in mycobacterial cording.
394 This is consistent with the fact that the rough colonial morphology relies primarily on the loss of
395 GPLs [22], which, like TPPs, are surface-exposed but structurally unrelated glycolipids.
396
397 TPPs are clearly required for infection of BPs and its derivatives as well as Muddy, with
398 important implications for clinical use, as both of these have been used therapeutically [4,5].
399 Moreover, Muddy and BPs are genomically distinct and share only seven genes with amino acid
400 sequence similarity, supporting their combined use in initial therapeutic cocktails on the basis of
401 likely different infection and thus different host resistance mechanisms. The finding that TPPs
402 are required for both phages and that co-resistance can occur by TPP loss, presents a counter
403 argument. Nonetheless, the ability of phage mutants with amino acid substitutions in the

404 predicted tail spike proteins of BPs (gp22) or Muddy (gp24) to overcome TPP-dependence
405 suggests that these should routinely replace their parent phages for therapeutic use. The spike
406 protein phage mutants reported here thus significantly expand the currently available repertoire
407 of therapeutic phages. Screening of a panel of phages in a TPP-defective mutant of *M.*
408 *smegmatis* show that TPPs are not generally required for phage infection, although several
409 additional phages also require TPPs.
410
411 A simple explanation for the role of TPPs is that they act as receptors for recognition by BPs
412 and Muddy and the other TPP-dependent phages, with phenotypes that are consistent with a
413 TPP requirement for adsorption to the cell surface. However, the finding that tail spike amino
414 acid substitutions readily overcome TPP-dependence would then need to be interpreted that
415 these can recognize a completely different receptor. Although this is plausible, it is unclear what
416 other surface molecules would present as being sufficiently structurally similar to TPPs for such
417 recognition. An alternative explanation is that TPPs are acting to facilitate interaction of the
418 phages with the actual phage receptor, and the tail spike mutants have gained the ability to bind
419 to the receptor without the aid of TPPs. This is consistent with the observation that tail spike
420 mutants such as phKSW1 adsorb substantially better than the parent phage even to TPP-
421 containing host cells and at least in *M. smegmatis*, adsorb better to a TPP-defective mutant than
422 wild-type phage to wild-type cells. Furthermore, wild-type BPs does not efficiently infect *M.*
423 *tuberculosis* H37Rv, but a mutant with the gp22 A604E substitution enables efficient infection [18],
424 even though *M. tuberculosis* lacks TPP [40]. Moreover, the ability of this phage mutant to infect *M.*
425 *tuberculosis* is specific to strain H37Rv, and it does not efficiently infect other *M. tuberculosis*
426 isolates [19]. Similarly, wild-type Muddy efficiently infects *M. tuberculosis* H37Rv [19] despite its lack
427 of TPPs, and Muddy tail spike substitutions expand its host range to other *M. tuberculosis*
428 strains [19]. These observations not only suggest that TPPs are not the receptors for these
429 phages *per se*, but that there may be general mechanisms governing receptor access by the

430 phages, together with phage strategies for expanding host cell recognition and infection.
431 Furthermore, if TPPs are not the target of direct phage recognition, the true receptor is likely to
432 be encoded by genes that are essential for mycobacterial viability, consistent with the lack of
433 transposon insertions in genes other than those influencing TPP production.
434
435 Globally, the roles of TPPs in phage infection are similar in *M. abscessus* and *M. smegmatis*.
436 Understanding the roles of TPP in *M. abscessus* is important for therapeutic phage use, and we
437 note that in at least some clinical isolates the loss of TPP through gene deletions or
438 translocation leads to loss of infection by BPs∆*33*HTH_HRM10 or Muddy. In the first therapeutic
439 use of mycobacteriophages, BPs∆*33*HTH_HRM10 and Muddy were used in combination with
440 ZoeJ, and it is of interest that ZoeJ does not display TPP-dependence. We also note that
441 resistance to BPs derivatives or Muddy has not been observed in clinical use, even in 11 cases
442 where Muddy was used alone [5]. It is plausible that resistance through TPP loss is not observed
443 due to loss of fitness and poor virulence as a notable tradeoff. The roles of TPP in *M. abscessus*
444 pathogenicity clearly needs further study. *M. smegmatis* provides a more genetically tractable
445 surrogate for studying the roles of TPP and its susceptibility to a large array of phages provides
446 opportunities for exploring phage-bacterium interactions.
447
448 Finally, transposon insertion mutagenesis used to isolate BPs∆*33*HTH_HRM10 and Muddy
449 resistant mutants identified insertions in TPP pathways synthesis/transport genes, as well as a
450 suite of other genes that appear to be also involved in TPP synthesis. The roles of these other
451 genes in synthesis or translocation of TPPs warrants further investigations. However, the finding
452 that all of the mutants isolated show loss of TPPs by TLC suggests that TPP loss is the sole
453 mechanism of resistance to these phages in *M. abscessus*. As such, if tail spike mutants of
454 BPs∆*33*HTH_HRM10 and Muddy are routinely used as substitutes of their parent phages in

455 therapeutic contexts, this may help to further minimize the likelihood of therapeutic failure due to
456 phage resistance.
457
458 **Acknowledgements**
459 We thank Chidiebere Akusobi, Mark Sullivan, Kerry McGowen, Carlos Rodriguez and William
460 DePas for helpful discussions. We also thank all of the students and faculty in the SEA-
461 PHAGES program that discovered and characterized phages used in this study, and the
462 numerous colleagues that provided *M. abscessus* strains in the GDxx series. Microscopy and
463 flow cytometry were performed at the Montpellier Imaging Center for Microscopy (MRI). This
464 work was supported by grants from the National Institutes of Health grants GM131729 and the
465 Howard Hughes Medical Institute Grant GT12053 to GFH, a Cystic Fibrosis Foundation Postdoc
466 Fellowship WETZEL21F0 to KSW, by the French National Research Agency ANR-21-CE44-
467 0027-01 (MYCOLT) to LK and CC and by Vaincre la Mucoviscidose (RF20200502678) and the
468 Association Grégory Lemarchal for funding the PhD fellowship of MI.
469
470 **Declaration of interests**
471
472 GFH receives support through a Collaborative Research Agreement with Janssen Inc., but
473 which did not fund the work reported here.
474
475

476 **Materials and Methods**

477 **Bacterial strains and culture conditions**

478 Bacterial strains (Table S1) were grown in Middlebrook 7H9 media (BD Difco) supplemented
479 10% oleic acid, albumin, dextrose, catalase (OADC enrichment) (7H9/OADC) or on Middlebrook
480 7H10/OADC solid media (BD Difco) at 37° C. Antibiotics were added when required.
481 Transformations of electrocompetent mycobacteria were performed using a Bio-Rad Gene
482 pulser (25 µF, 2500 V, 800 Ohms). For some *M. smegmatis* strains, Tween-80 (0.05%) was
483 used in starter cultures but omitted in subcultures used for phage infections. Cultures used in
484 phage infection were supplemented with 1 mM $CaCl_2$. When required, *M. abscessus* strains
485 were selected with 1 mg/mL hygromycin or 200 µg/mL streptomycin. *M. abscessus* strains in the
486 GDxx series are part of strain collection at the University of Pittsburgh and were kindly provided
487 by numerous colleagues.

488

489 **Engineering of MycoMarT7-Hyg2**

490 Phage MycoMarT7-Hyg1 and MycoMarT7-Hyg2 were engineered from phage MycoMarT7
491 using CRISPY-BRED recombineering [31]. Briefly, dsDNA recombineering substrates were
492 designed that contained the desired mutation (a HygR cassette) with flanking sequence to
493 permit the replacement of either KanR (MycoMarT7-Hyg1) or KanR and oriR6K (MycoMarT7-
494 Hyg2). These substrates and genomic DNA from MycoMarT7 were transformed into *M.*
495 *smegmatis* mc^2155 recombineering cells that contain the plasmid pJV138 [31]. Transformations
496 were combined with cells containing a CRISPR plasmid selecting against the parent
497 MycoMarT7 and plated on solid media; this enriches mutants containing the allelic replacement
498 that form plaques on the plate. Resulting plaques were screened for presence of the Hyg-
499 marked transposon by PCR, and positive plaques were plaque purified, whole genome
500 sequenced, and confirmed to have retained temperature sensitivity.

501

502 **Construction of the *M. abscessus* GD01 transposon insertion library and phage**
503 **challenge**
504 The transposon mutagenesis library was largely prepared as previously described [32]. Briefly, 50
505 mL of *M. abscessus* GD01 was grown to an OD_{600} of 0.2. The cells were pelleted and
506 resuspended in 1 mL of phage buffer (10 mM Tris HCl, pH 7.5; 10 mM $MgSO_4$; 68.5 mM NaCl; 1
507 mM $CaCl_2$), pre-warmed to 37° C and infected with 800 µL MycoMarT7-Hyg2 ($5x10^{10}$ pfu/mL).
508 The cells and MycoMarT7-Hyg2 were incubated at 37° C for 7.5 hours. Cells were pelleted and
509 resuspended in 8 mL PBS + 0.05% Tween80, and the resuspension was combined with 8 mL
510 40% glycerol for freezing at -80° C. The transduction frequency was determined by measuring
511 hygromycin resistant colonies/mL and 120,000 transductants were plated onto large square
512 plates containing solid 7H10 media with 0.1% Tween80 and 1 mg/mL hygromycin. Plates
513 incubated at 37° C for nine days. To harvest the library, cells were scraped off the solid media,
514 resuspended in 7H9/OADC combined with 40% glycerol, aliquoted and frozen at -80° C.
515
516 To identify GD01 insertion mutants that were resistant to phage infection, ~20 µL of GD01 Tn
517 library was thawed and grown overnight to an OD600 of 0.175. Dilutions of this culture
518 (approximately 10^4, 10^5 and 10^6 cells) were spread onto 7H10 solid media plates seeded with or
519 without 10^8 pfu of phages BPs_Δ*33*HTH_HRM10 or Muddy. Plates were incubated at 37° C for
520 seven days. Colonies able to grow on phage seeded plates were subjected to PCR to identify a
521 transposon insertion site (see below) and struck out two times to remove any remaining phage.
522 After streaking, single colonies were grown in liquid media and used for phage susceptibility
523 testing by standard plaque assay.
524
525 **Identification of transposon insertion sites**
526 Transposon insertion sites were identified by PCR using a primer that annealed to the
527 transposon in the hygromycin resistance gene (Tn_Hyg_Fwd_2: 5'-

528 CTTCACCTTCCTGCACGACT-3'), and a primer with a degenerate 3' end, or if that did not yield
529 an amplicon, nested PCR with primers Tn_Hyg_Fwd_2 and Primer 557 (5'-
530 GGCCAGCGAGCTAACGAGCANNNNNNNGTT-3') followed by PCR with primers Primer 414
531 (5'-GGCCAGCGAGCTAACGAGAC-3') and Tn_Hyg_Fwd_1 (5'-
532 TTCGAGGTGTTCGAGGAGAC-3'). Amplicons were gel extracted, Sanger sequenced from the
533 transposon, and the result aligned to the GD01 sequence to identify the transposon insertion
534 site. For most strains (and at least one strain per interrupted gene), the transposon insertion site
535 was confirmed by designing primers that flanked the site identified by the initial PCR and
536 confirming that this region had increased in size by 1,259 bp compared to strain GD01.
537

538 **Screening of phage susceptibility**

539 Phage susceptibility profiles were assessed using standard plaque assays. Top agar bacterial
540 lawns were made by combining Middlebrook Top Agar (MBTA; Middlebrook 7H9, 1 mM $CaCl_2$,
541 0.35% BactoAgar) with 300 µL-500 µL cell culture. After top agar had solidified, phages were
542 10-fold serially diluted and spotted onto the top agar bacterial lawns and incubated 24-48 hours
543 (*M. smegmatis*) or 5-7 days (*M. abscessus*) until bacterial lawns were confluent. Phages used
544 in this study were obtained from University of Pittsburgh and *M. smegmatis* mc^2155 was used to
545 propagate them.
546

547 **Plasmid construction**

548 To create plasmid pKSW131, *fadD23*, *pE*, *mmpL10* and *papA3* and the flanking intergenic
549 sequence was amplified using Q5 HiFi 2× MasterMix (NEB) from genomic DNA isolated from *M.*
550 *abscessus* GD01. The amplicon was purified and cloned into EcoRI-digested vector pLA155
551 using the NEBuilder Gibson Assembly Master Mix and transformed into *E. coli* strain DH5a. The
552 culture that yielded a successfully constructed plasmid was grown at 30° C rather than 37° C,
553 although it is unknown if this contributed to successful plasmid maintenance in the culture. To

554 create plasmid pKSW134, the open reading frame of *fadD23* was amplified from GD01 gDNA
555 and cloned into Pml I-digested anhydrotetracycline (ATc) inducible vector pCCK39 [41] using the
556 NEBuilder Gibson Assembly Master Mix. The entire plasmids were sequenced by
557 Plasmidsaurus Inc (https://www.plasmidsaurus.com/).
558
559 pMV*pks_mWasabi* and pMV*mmpL10_mWasabi* were constructed based on pMV*pks* and
560 pMV*mmpL10* by in-fusion cloning. The *mWasabi* sequence under the control of the constitutive
561 *Pleft** promoter [42] was amplified by PCR using a Q5 high-fidelity DNA polymerase (New
562 England Biolabs). Plasmids were linearized with Kpn I-HF (New England Biolabs). Agarose gels
563 were used to purify linear fragments, then circularized using In-Fusion SNAP Assembly Master
564 Mix (Takara Inc.), according to the manufacturer's instructions. Stellar competent cells were
565 used for transformation. Plasmids generated were verified by sequencing.
566
567 **Isolation and whole genome sequencing of phage resistant mycobacteria mutants**
568 Two of these phage resistant mutants (GD17_RM1 and GD22 RM_4) were described previously
569 [9]; the others were isolated in the same manner. Briefly, 10^8 CFU *M. abscessus* were incubated
570 with 10^9 PFU of phage. Infections were plated on solid media at two and five days post infection,
571 and survivors were purified, tested for phage resistance, and sequenced. The mutants were
572 sequenced as were described previously [9].
573
574 **Isolation of BPs_Δ*33*HTH_HRM10 mutants**
575 Clear plaques were observed within high titer spots for phage BPs_Δ*33*HTH_HRM10 on strains
576 GD01Tn_BPs_HRM10_RM6, GD01Tn_BPs_HRM10_RM11 and GD180_RM2. These plaques
577 were picked and plated on the resistant strain two additional times to purify. A purified plaque
578 was then used to produce a high-titer phage lysate on *M. smegmatis* mc^2155, and subsequently
579 subjected to gene *22* PCR sequencing or whole-genome sequencing.

580

581 **Total lipids extraction of mycobacteria and TLC analysis**

582 Bacteria were grown in LB medium at 37° C without agitation and pelleted by centrifugation
583 (3,000 *g*, 10 min, room temperature). Lipids were extracted as described previously [23]. Briefly,
584 bacterial pellets were treated successively with $CHCl_3/CH_3OH$ (1:2) and $CHCl_3/CH_3OH$ (2:1),
585 washed with water and dried. Lipids were resuspended in $CHCl_3$ prior to spot on TLC. For TLC
586 analysis, silica gel G60 plates (10 x 20 cm, Macherey-Nagel) were used to spot samples and
587 lipids were separated with $CHCl_3/CH_3OH$ (90:10, v/v). Lipid profiles were shown by spraying the
588 plates with a 0.2% anthrone solution (w/v) in concentrated H_2SO_4 and charring.

589

590 **Adsorption Assays**

591 *M. smegmatis* strains were grown to an OD_{600} of 0.5-0.8, then concentrated approximately
592 tenfold to $1.75x10^9$/mL. One milliliter of cells (*M. smegmatis* mc^2155 or mc^2155 Δ*pks*) were
593 infected in triplicate in a 12-well plate at a multiplicity of infection (MOI) of 0.001. At each
594 timepoint, 50 µL of liquid were removed, pelleted, and the supernatant that contained unbound
595 phage was titered on *M. smegmatis*. For *M. abscessus* GD01 and *M. abscessus* GD01
596 *fadD23*::Tn, the same protocol was followed but the strains were grown to an OD_{600} of 0.15-0.25
597 and cells were concentrated approximately tenfold to $6.3x10^8$/mL.

598

599 **Growth curves of mycobacteria incubated with phages**

600 Bacterial growth assays were performed in 96-well plates (Falcon), each well containing 100 µL
601 of bacterial culture and 100 µL of phage lysates or medium as control. Exponential phage
602 cultures of mycobacteria were used and set at $3x10^7$ CFU/mL in Middlebrook 7H9/OADC
603 supplemented with 1 mM $CaCl_2$. Phages were incubated at a MOI 10 and diluted in 7H9/OADC
604 supplemented with 1 mM $CaCl_2$. Measurements were taken every three hours for *M. smegmatis*
605 strains and six hours for *M. abscessus* strains with a spectrophotometer (Tecan, infinite 200

606 PRO) until stationary phase was reached (2 days for *M. smegmatis* strains and 6 days for *M.*
607 *abscessus* strains). Plates were incubated at 37° C without agitation.
608
609 **Microscopy and flow cytometry sample preparation**
610 Mycobacteria were sub-cultured in 7H9/OADC with agitation to obtain exponential phase
611 cultures. Bacteria were concentrated to obtain a sample containing $1.2x10^7$ CFU (for
612 microscopy) or $6x10^6$ CFU (for flow cytometry) and then incubated with either medium or phage
613 BPs_Δ*33*HTH_HRM10 as controls or phage BPs_Δ*33*HTH_HRM10 mCherry (MOI 10). For *M.*
614 *smegmatis* strains, the infections were performed for two hours and four hours for *M. smegmatis*
615 and *M. abscessus*, respectively, at 37° C without agitation. After infection, samples were fixed
616 with PFA 4% for 20 min at room temperature. Samples were then diluted as necessary
617 depending on the experiment with 7H9/OADC supplemented with 0.025% tyloxapol and
618 sonicated to disrupt bacterial aggregates. For microscopy, samples were then mounted
619 between coverslips and slides with Immu-Mount (Epredia). Samples were kept at 4° C in the
620 dark until analysis.
621
622 **Microscopy**
623 DIC (Differential interference contrast) and epifluorescence images were acquired on a ZEISS
624 Axio Imager Z1 up-right microscope. A 63X Plan Apochromat 1.4 NA oil objective and a 100X
625 Plan Apochromat 1.4 NA oil objective was used respectively for *M. smegmatis* or *M. abscessus*
626 strains. mCherry was excited with an Intenslight fiber lamp with Texas Red (Ex: 560/40, dic.
627 585, Em: 630/75) filter cube. Images were acquired with a scMOS ZYLA 4.2 MP.
628
629 **Image analysis**
630 Representative fields without technical artefacts were chosen. Fiji software was used to adjust
631 intensity, brightness and contrast (identically for compared image sets).

632

633 **Flow cytometry**

634 Infected bacteria were analysed by flow cytometry using a NovoCyte ACEA flow cytometer
635 (excitation laser wavelength: 561 nm, emission filter: 615/20 nm). Gates were drawn using SSC-
636 A/FSC-A and multiple cells were excluded with SSC-H / SSC-A. Uninfected cells and bacteria
637 infected by non-fluorescent phage were included as controls. Approximately 300,000 events
638 were recorded per experiment. Analysis was done with NovoExpress.

639

640 **Statistical analysis**

641 Statistical analysis was carried out with GraphPad Prism version 9.0.0 for Windows (GraphPad
642 Software, San Diego, California, United States). Descriptive statistics are cited and represented
643 as median and interquartile range for each of the variables calculated. A non-parametric Dunn's
644 test was used to compare the different conditions at 48 hours for *M. smegmatis* or 144 hours for
645 *M. abscessus*. A significance level *a priori* was set at $\alpha = 0.05$.

646

647 **Phylogenetic analysis of TPP pathway amino acid sequences in *M. abscessus***

648 A phylogenetic tree was constructed of a concatenated alignment of amino acid sequences of
649 the five TPP synthesis pathway members for 143 clinical isolates of *M. abscessus* and *M.*
650 *abscessus* ATCC19977. Homologs were identified using MMSeqs2 and phammseqs [43] and
651 subsequently aligned using ClustalO and Trimal [44]. A concatenated alignment was generated
652 with a custom python script and the maximum likelihood phylogeny was generated using
653 RAxML [45].

654

655

656 **References**

657 1. Martiniano, S.L., Nick, J.A. & Daley, C.L. Nontuberculous Mycobacterial Infections in Cystic
658 Fibrosis. *Thorac Surg Clin* **29**, 95-108 (2019).
659 2. Johansen, M.D., Herrmann, J.L. & Kremer, L. Non-tuberculous mycobacteria and the rise of
660 Mycobacterium abscessus. *Nat Rev Microbiol* **18**, 392-407 (2020).
661 3. Nick, J.A., Daley, C.L., Lenhart-Pendergrass, P.M. & Davidson, R.M. Nontuberculous
662 mycobacteria in cystic fibrosis. *Curr Opin Pulm Med* **27**, 586-592 (2021).
663 4. Dedrick, R.*, et al.* Engineered bacteriophages for treatment of a patient with a disseminated
664 drug-resistant *Mycobacterium abscessus*. *Nature Medicine* **25**, 730-733 (2019).
665 5. Dedrick, R.M.*, et al.* Phage Therapy of Mycobacterium Infections: Compassionate-use of
666 Phages in Twenty Patients with Drug-Resistant Mycobacterial Disease. *Clin Infect Dis*,
667 ciac453 (2022).
668 6. Nick, J.A.*, et al.* Host and pathogen response to bacteriophage engineered against
669 Mycobacterium abscessus lung infection. *Cell* **185**, 1860-1874 e1812 (2022).
670 7. Little, J.S.*, et al.* Bacteriophage treatment of disseminated cutaneous Mycobacterium
671 chelonae infection. *Nat Commun* **13**, 2313 (2022).
672 8. Hatfull, G.F. Mycobacteriophages: From Petri dish to patient. *PLoS Pathog* **18**, e1010602
673 (2022).
674 9. Dedrick, R.M.*, et al.* Mycobacterium abscessus Strain Morphotype Determines Phage
675 Susceptibility, the Repertoire of Therapeutically Useful Phages, and Phage Resistance.
676 *mBio* **12**(2021).
677 10. Hatfull, G.F., Dedrick, R.M. & Schooley, R.T. Phage Therapy for Antibiotic-Resistant
678 Bacterial Infections. *Annu Rev Med* **73**, 197-211 (2022).
679 11. Hatfull, G.F. Actinobacteriophages: Genomics, Dynamics, and Applications. *Annu Rev Virol*
680 **7**, 37-61 (2020).

681 12. Chen, J.*, et al.* Defects in glycopeptidolipid biosynthesis confer phage I3 resistance in
682 Mycobacterium smegmatis. *Microbiology* **155**, 4050-4057 (2009).
683 13. Russell, D.A. & Hatfull, G.F. PhagesDB: the actinobacteriophage database. *Bioinformatics*
684 **33**, 784-786 (2017).
685 14. Pedulla, M.L.*, et al.* Origins of highly mosaic mycobacteriophage genomes. *Cell* **113**, 171-
686 182 (2003).
687 15. Pope, W.H.*, et al.* Whole genome comparison of a large collection of mycobacteriophages
688 reveals a continuum of phage genetic diversity. *Elife* **4**, e06416 (2015).
689 16. Hatfull, G.F.*, et al.* Comparative Genomic Analysis of 60 Mycobacteriophage Genomes:
690 Genome Clustering, Gene Acquisition, and Gene Size. *J Mol Biol* **397**, 119-143 (2010).
691 17. Hatfull, G.F.*, et al.* Exploring the mycobacteriophage metaproteome: phage genomics as an
692 educational platform. *PLoS Genet* **2**, e92 (2006).
693 18. Jacobs-Sera, D.*, et al.* On the nature of mycobacteriophage diversity and host preference.
694 *Virology* **434**, 187-201 (2012).
695 19. Guerrero-Bustamante, C.A., Dedrick, R.M., Garlena, R.A., Russell, D.A. & Hatfull, G.F.
696 Toward a Phage Cocktail for Tuberculosis: Susceptibility and Tuberculocidal Action of
697 Mycobacteriophages against Diverse Mycobacterium tuberculosis Strains. *mBio* **12**(2021).
698 20. Abrahams, K.A. & Besra, G.S. Synthesis and recycling of the mycobacterial cell envelope.
699 *Curr Opin Microbiol* **60**, 58-65 (2021).
700 21. Gutierrez, A.V., Viljoen, A., Ghigo, E., Herrmann, J.L. & Kremer, L. Glycopeptidolipids, a
701 Double-Edged Sword of the Mycobacterium abscessus Complex. *Front Microbiol* **9**, 1145
702 (2018).
703 22. Bernut, A.*, et al.* Insights into the smooth-to-rough transitioning in Mycobacterium bolletii
704 unravels a functional Tyr residue conserved in all mycobacterial MmpL family members.
705 *Mol Microbiol* **99**, 866-883 (2016).

706 23. Burbaud, S., *et al.* Trehalose Polyphleates Are Produced by a Glycolipid Biosynthetic
707 Pathway Conserved across Phylogenetically Distant Mycobacteria. *Cell Chem Biol* **23**, 278-
708 289 (2016).
709 24. Llorens-Fons, M., *et al.* Trehalose Polyphleates, External Cell Wall Lipids in Mycobacterium
710 abscessus, Are Associated with the Formation of Clumps with Cording Morphology, Which
711 Have Been Associated with Virulence. *Front Microbiol* **8**, 1402 (2017).
712 25. Thouvenel, L., *et al.* The final assembly of trehalose polyphleates takes place within the
713 outer layer of the mycobacterial cell envelope. *J Biol Chem* **295**, 11184-11194 (2020).
714 26. Hatfull, G.F. Phage Therapy for Nontuberculous Mycobacteria: Challenges and
715 Opportunities. *Pulm Ther* **9**, 91-107 (2023).
716 27. Dedrick, R.M., *et al.* Mycobacteriophage ZoeJ: A broad host-range close relative of
717 mycobacteriophage TM4. *Tuberculosis (Edinb)* **115**, 14-23 (2019).
718 28. Sampson, T., *et al.* Mycobacteriophages BPs, Angel and Halo: comparative genomics
719 reveals a novel class of ultra-small mobile genetic elements. *Microbiology* **155**, 2962-2977
720 (2009).
721 29. Majumdar, G., *et al.* Genome-Wide Transposon Mutagenesis in Mycobacterium
722 tuberculosis and Mycobacterium smegmatis. *Methods Mol Biol* **1498**, 321-335 (2017).
723 30. Johansen, M.D., *et al.* Mycobacteriophage-antibiotic therapy promotes enhanced clearance
724 of drug-resistant Mycobacterium abscessus. *Dis Model Mech* **14**(2021).
725 31. Wetzel, K.S., *et al.* CRISPY-BRED and CRISPY-BRIP: efficient bacteriophage engineering.
726 *Sci Rep* **11**, 6796 (2021).
727 32. Akusobi, C., *et al.* Transposon mutagenesis in Mycobacterium abscessus identifies an
728 essential penicillin-binding protein involved in septal peptidoglycan synthesis and antibiotic
729 sensitivity. *Elife* **11**(2022).
730 33. McKitterick, A.C. & Bernhardt, T.G. Phage resistance profiling identifies new genes required
731 for biogenesis and modification of the corynebacterial cell envelope. *Elife* **11**(2022).

732 34. Bohm, K.*, et al.* Genes affecting progression of bacteriophage P22 infection in Salmonella
733 identified by transposon and single gene deletion screens. *Mol Microbiol* **108**, 288-305
734 (2018).
735 35. Mutalik, V.K.*, et al.* High-throughput mapping of the phage resistance landscape in E. coli.
736 *PLoS Biol* **18**, e3000877 (2020).
737 36. Kortright, K.E., Chan, B.K. & Turner, P.E. High-throughput discovery of phage receptors
738 using transposon insertion sequencing of bacteria. *Proc Natl Acad Sci U S A* **117**, 18670-
739 18679 (2020).
740 37. Rifat, D., Chen, L., Kreiswirth, B.N. & Nuermberger, E.L. Genome-Wide Essentiality
741 Analysis of Mycobacterium abscessus by Saturated Transposon Mutagenesis and Deep
742 Sequencing. *mBio* **12**, e0104921 (2021).
743 38. Dulberger, C.L.*, et al.* Mycobacterial nucleoid-associated protein Lsr2 is required for
744 productive mycobacteriophage infection. *Nat Microbiol* (2023).
745 39. Judd, J.A.*, et al.* A Mycobacterial Systems Resource for the Research Community. *mBio*
746 **12**(2021).
747 40. Touchette, M.H.*, et al.* The rv1184c locus encodes Chp2, an acyltransferase in
748 Mycobacterium tuberculosis polyacyltrehalose lipid biosynthesis. *J Bacteriol* **197**, 201-210
749 (2015).
750 41. Ko, C.C. & Hatfull, G.F. Mycobacteriophage Fruitloop gp52 inactivates Wag31 (DivIVA) to
751 prevent heterotypic superinfection. *Mol Microbiol* **108**, 443-460 (2018).
752 42. Nesbit, C.E., Levin, M.E., Donnelly-Wu, M.K. & Hatfull, G.F. Transcriptional regulation of
753 repressor synthesis in mycobacteriophage L5. *Mol Microbiol* **17**, 1045-1056 (1995).
754 43. Gauthier, C.H., Cresawn, S.G. & Hatfull, G.F. PhaMMseqs: a new pipeline for constructing
755 phage gene phamilies using MMseqs2. *G3 (Bethesda)* **12**(2022).

756 44. Capella-Gutierrez, S., Silla-Martinez, J.M. & Gabaldon, T. trimAl: a tool for automated
757 alignment trimming in large-scale phylogenetic analyses. *Bioinformatics* **25**, 1972-1973
758 (2009).
759 45. Stamatakis, A., Ludwig, T. & Meier, H. RAxML-III: a fast program for maximum likelihood-
760 based inference of large phylogenetic trees. *Bioinformatics* **21**, 456-463 (2005).
761 46. Bachmann, B.O. & Ravel, J. Chapter 8. Methods for in silico prediction of microbial
762 polyketide and nonribosomal peptide biosynthetic pathways from DNA sequence data.
763 *Methods Enzymol* **458**, 181-217 (2009).
764

765 **Figure Legends**

766

767 **Figure 1. Identification of phage-resistant transposon insertion mutants of *M. abscessus***
768 **GD01**. **A**. Construction of MycoMarT7-Hyg1 and MycoMarT7-Hyg2. Transposon delivery phage
769 phiMycoMarT7 delivers a Transposon containing *Escherichia coli* ori6Kγ (grey) and kanamycin
770 resistance cassette (blue), flanked by 29 bp inverted repeats (yellow boxes). CRISPY-BRED [31]
771 was used to create phiMycoMarT7-Hyg1 and phiMycoMarT7-Hyg2, which deliver transposons
772 containing oriR6K (grey box) and a hygromycin resistance cassette (red box), or only a
773 hygromycin resistance cassette. **B**. *M. abscessus* GD01 or a transposon library of *M. abscessus*
774 strain GD01 (GD01 Tn Lib) were plated on solid media or solid media seeded with phages
775 BPs_Δ*33*HTH_HRM10. **C**. Locations of transposon insertions in the TPP locus in phage
776 resistant mutants. Red and black circles show mutants isolated as resistant to BPs and Muddy,
777 respectively; filled and open circles reflect insertions in forward and reverse orientations. **D**.
778 Proposed roles of Pks, PapA3, FadD23, MmpL10 and PE in the synthesis and transport of TPP
779 and DAT. **E**. Tenfold serial dilutions of phages were spotted onto solid media with *M. smegmatis*
780 mc^2155, *M. abscessus* GD01, or representative *M. abscessus* GD01 transposon insertion
781 mutant strains: GD01 f*adD23*::Tn (GD01Tn_BPs_HRM10_RM1); GD01 *pE*::Tn
782 (GD01Tn_BPs_HRM10_RM6); GD01 *mmpL10*::Tn (GD01Tn_BPs_HRM10_RM11); GD01
783 *papA3*::Tn , (GD01Tn_BPs_HRM10_RM10). **F**. Tenfold serial dilutions of phages were spotted
784 onto solid media with strain GD01 *fadD23*::Tn/(BPs_HRM10_RM1) containing plasmid
785 pKSW134, which contains gene *fadD23* under expression of an anhydrotetracycline (ATc)-
786 inducible promoter. FadD23 is not expressed in the absence of ATc (left panel) but is induced
787 by ATc (right panel).

788

789 **Figure 2. Transposon insertion mutants are deficient in trehalose polyphleates. A.** TLC
790 analysis of total lipids extracted *M. abscessus* GD01 and mutants with transposon insertions in

791 the known TPP synthesis and transport genes. *M. smegmatis* mc^{2}155 and a Δ*mmpL10* mutant
792 strain of *M. smegmatis* are also included as controls. **B**. TLC analysis of total lipids extracted
793 from *M. abscessus* GD01 and phage resistant mutants with transposon insertions in gene not
794 previously shown to be involved in TPP synthesis or transport. *M. smegmatis* mc^{2}155 and a
795 Δ*mmpL10* mutant strain of *M. smegmatis* are also shown. **C**. Ten-fold serial dilutions of phage
796 lysates (as indicated on left) were spotted onto solid media with either the parent *M. abscessus*
797 strains (left column) or transposon insertion mutant strains. All transposon insertion strains
798 showed the same infection profiles and two representative strains are shown (M. ab. GD01
799 *MAB_3593*::Tn is GD01Tn_BPsHRM10_RM5; M. ab. GD01 *MAB_2081*::Tn is
800 GD01Tn_BPsHRM10_RM19).
801
802 **Figure 3. Mutants of BPs_Δ*33*HTH_HRM10 and Muddy overcome TPP loss. A**. Ten-fold
803 serial dilutions of BPs_Δ*33*HTH_HRM10 and gp22 mutants (as indicated on left) were spotted
804 onto solid media with *M. smegmatis* mc^{2}155, *M. abscessus* GD01, or *M. abscessus* GD01
805 transposon insertion mutant strains (top panels). The locations of amino acid substitutions in
806 BPs_Δ*33*HTH_HRM10 gp22 conferring the ability to infect TPP deficient strains (red) or were
807 previously found to broaden host range to include *M. tuberculosis* (purple) (bottom panel). The
808 A306V and A604E substitutions were identified with both assays. **B**. Adsorption of phages
809 BPs_Δ*33*HTH_HRM10, phKSW1 and ZoeJΔ*43-45* to *M. abscessus* strains GD01 and GD01
810 *fadD23*::Tn as indicated by the percentage of unadsorbed phages remaining in infection
811 supernatants at different times after infection. Assays were performed in duplicate at least twice
812 with similar results and a representative experiment is shown. **C**. Tenfold serial dilutions of
813 Muddy and Muddy gp24 mutants (as indicated on left) were spotted onto solid media with *M.*
814 *smegmatis* mc^{2}155, *M. abscessus* GD01, or *M. abscessus* GD01 transposon insertion mutant

815 strains (top panels). The location of amino acid substitutions in Muddy gp24 that confer the
816 ability to infect TPP deficient strains (bottom panel).
817
818 **Figure 4. Phage infection profiles of *M. abscessus* spontaneous phage resistant mutants**.
819 Tenfold serial dilutions of phage lysates (as indicated on left) were spotted onto solid media with
820 *M. smegmatis* mc^2155, the parent *M. abscessus* strains (left) or spontaneously isolated phage
821 resistant mutant (RM) derivatives (right). **B**. A schematic representation of *M. abscessus* Pks
822 showing the location of predicted functional domains and the amino acid changes in
823 spontaneous phage resistant mutants below. Domain abbreviations are: AT, Acyltransferase;
824 KS, Ketosynthase, KR, Ketoreductase; DH, Dehydratase; ER, Enoylreductase; PP,
825 phosphopantetheinylate acyl carrier protein. Domains were identified using the PKS analysis
826 web site at http://nrps.igs.umaryland.edu/ [46].
827
828 **Figure 5. TPPs are essential for BPs_Δ*33*HTH_HRM10 to lyse *M. abscessus*. A**.
829 Representation of the *M. abscessus* TPP locus showing the mutations affecting the clinical
830 strains studied. **B**.TLC analysis of total lipids extracted from *M. abscessus* clinical strains (GD22
831 and GD180), spontaneous resistant mutants (RM) and complemented strains (::C). Eluent:
832 $CHCl_3/CH_3OH$ (90:10, v/v). Anthrone was sprayed on the plates to visualized the lipid profile
833 and followed by charring. **C**. Phage efficiency on solid media against clinical strains, resistant
834 mutants and complemented strains. Phages were spotted as ten-fold serial dilutions. Plates
835 were incubated 2-3 days at 37° C prior to image. The assay was repeated at least three times
836 and a representative experiment is shown. **D**. Liquid growth of the strains with or without
837 BPs_Δ*33*HTH_HRM10 or BPs_Δ*33*HTH_HRM10 mCherry (MOI 10) monitored every 6 hours for
838 6 days at 37° C in $7H9^{OADC}$ supplemented with 1 mM $CaCl_2$. Data are plotted as the median of
839 three independent experiments made in triplicates ± interquartile range. Statistical analysis
840 conducted to compare the differences at 144h between each strain. ns, $P \geq 0.05$, * $P \leq 0.05$, **

841 P ≤ 0.01, *** P ≤ 0.001**** P ≤ 0.0001. **E**. Representative fields of *M. abscessus* clinical strains
842 infected with BPs_Δ*33*HTH_HRM10 mCherry (MOI 10) for 4 hours at 37° C prior to fixation.
843 Infected bacilli appear in red. **F**. Flow cytometry data are represented as dot plot show the
844 percentage of bacilli infected with the BPs_Δ*33*HTH_HRM10 mCherry fluorophage relative to
845 the study population.
846
847 **Figure 6**. **TPP synthesis pathway gene variation and phage infection. A**. Amino acid
848 sequences from the five TPP synthesis pathway genes (shown in panel B) in 143 *M. abscessus*
849 clinical isolates (and *M. abscessus* ATCC19977) were concatenated and used to construct a
850 phylogenetic tree. Strain morphotype is labeled as either R for rough or S for
851 smooth. Susceptibilities to phages BPs_Δ*33*HTH_HRM10 and Muddy are represented in green
852 and red, as described previously [9]. Arrows indicate strains in panels B and C. **B**. Position of the
853 large deletions (GD262 and GD273) or insertions (GD155 and GD286) in the *pks* gene with
854 respect to the GD01 TPP locus. **C**. Ten-fold serial dilutions of phage lysates (as indicated on
855 left) were spotted onto solid media with either *M. smegmatis* mc^2155 or *M. abscessus* strains
856 GD273 and GD286. The control BPsΔ*33*HTH_HRM10 and BPsREM1 phage spots on *M.*
857 *smegmatis* are from the same experiment.
858
859 **Figure 7. TPPs are also required for infection of *M. smegmatis* by phages BPs and**
860 **Muddy. A**. Tenfold serial dilutions of phages (as indicated on left) were spotted onto solid media
861 with *M. smegmatis* mc^2155, Δ*pks*, Δ*papA3* or Δ*fadD23* as indicated. **B**. TLC analysis of total
862 lipids extracted from wild-type *M. smegmatis*, three TPP-deficient mutants and the
863 corresponding complemented strains. Eluent: $CHCl_3/CH_3OH$ (90:10, v/v). TLC was revealed by
864 spraying anthrone on the plate, followed by charring. **C**. Adsorption of phages
865 BPs_Δ*33*HTH_HRM10, phKSW1 and ZoeJΔ*43-45* on *M. smegmatis* strains mc^2155 and Δ*pks*
866 as indicated by the percentage of unadsorbed phages remaining in infection supernatant at

867 different times after infection. Assays were performed in triplicate at least twice with similar

868 results and a representative experiment is shown. **D**. A panel of phages from various genetic

869 clusters were tenfold serially diluted and spotted onto *M. smegmatis* mc^2155 and Δ*pks.* Phage

870 names are shown with their cluster/subcluster designation in parentheses.

871

Table 1. Characterization of phage resistant *M. abscessus* GD01 transposon mutants

Strain Name[1]	Isolated as resistant to[2]	Tn insertion coordinate[3]	Direction of Hyg ORF[4]	GD01 Locus Tag[5]	ATCC19977 Gene Name[6]	Protein Name/ Function Prediction[7]	PCR ver.[8]	Plaque assay[9]
GD01Tn_BPsHRM10_RM18	BPs	50130	Fwd	EXM25_00255	*MAB_0457*	Hypothetical protein	Y	Y
GD01Tn_Muddy_RM9	Muddy	895811	Rev	EXM25_04535	*MAB_0935c*	FadD23	Y	Y
GD01Tn_BPsHRM10_RM9	BPs	896103	Fwd	EXM25_04535	*MAB_0935c*	FadD23	ND	ND
GD01Tn_BPsHRM10_RM15	BPs	896250	Rev	EXM25_04535	*MAB_0935c*	FadD23	ND	ND
GD01Tn_Muddy_RM11[10]	Muddy	896372	Rev	EXM25_04535	*MAB_0935c*	FadD23	ND	ND
GD01Tn_Muddy_RM15[10]	Muddy	896372	Rev	EXM25_04535	*MAB_0935c*	FadD23	ND	ND
GD01Tn_Muddy_RM13	Muddy	896513	Rev	EXM25_04535	*MAB_0935c*	FadD23	ND	ND
GD01Tn_Muddy_RM7	Muddy	896840	Rev	EXM25_04535	*MAB_0935c*	FadD23	ND	ND
GD01Tn_Muddy_RM12	Muddy	896990	Rev	EXM25_04535	*MAB_0935c*	FadD23	Y	Y
GD01Tn_BPsHRM10_RM1	BPs	897275	Rev	EXM25_04535	*MAB_0935c*	FadD23	Y	Y
GD01Tn_BPsHRM10_RM6	BPs	897828	Rev	EXM25_04540	*MAB_0936c*	PE	Y	Y
GD01Tn_Muddy_RM20	Muddy	898646	Rev	EXM25_04540	*MAB_0936c*	PE	Y	Y
GD01Tn_BPsHRM10_RM11	BPs	899212	Fwd	EXM25_04545	*MAB_0937c*	Mmpl10	Y	Y
GD01Tn_BPsHRM10_RM2	BPs	901937	Rev	EXM25_04550	*MAB_0938c*	PapA3	ND	ND
GD01Tn_Muddy_RM17	Muddy	902798	Fwd	EXM25_04550	*MAB_0938c*	PapA3	Y	Y
GD01Tn_BPsHRM10_RM10	BPs	902799	Rev	EXM25_04550	*MAB_0938c*	PapA3	Y	Y
GD01Tn_Muddy_RM19	Muddy	903001	Rev	EXM25_04550	*MAB_0938c*	PapA3	Y	Y
GD01Tn_BPsHRM10_RM13	BPs	934573	Rev	EXM25_04650	*MAB_0958c*	NAD(P)-binding domain-containing protein	Y	Y
GD01Tn_BPsHRM10_RM3	BPs	1702803	Rev	EXM25_08515	*MAB_1681*	Hypothetical protein	Y	Y
GD01Tn_Muddy_RM6	Muddy	1799970	Fwd	EXM25_09000	*MAB_1882c*	DoxX family membrane protein	Y	Y
GD01Tn_BPsHRM10_RM19	BPs	2004769	Rev	EXM25_10050	*MAB_2081*	Acyl-CoA dehydrogenase family protein	Y	Y
GD01Tn_Muddy_RM14	Muddy	2068078	Fwd	EXM25_10305	*MAB_2130*	HAD family phosphatase	Y	Y
GD01Tn_BPsHRM10_RM17	BPs	3319297	Rev	EXM25_16510	*MAB_3332c*	DoxX family protein	Y	Y
GD01Tn_BPsHRM10_RM14	BPs	3419195	Rev	EXM25_17025	*MAB_3426c*	SDR family oxidoreductase	Y	Y
GD01Tn_BPsHRM10_RM4	BPs	3438375	Fwd	EXM25_17140	*MAB_3449c*	MFS transporter	Y	Y
GD01Tn_BPsHRM10_RM7[10]	BPs	3546108	Rev	EXM25_17670/ 17675 IR	*MAB_3538/ 3539 IR*		Y	Y
GD01Tn_BPsHRM10_RM12[10]	BPs	3546108	Rev	EXM25_17670/ 17675 IR	*MAB_3538/ 3539 IR*		ND	ND
GD01Tn_BPsHRM10_RM5	BPs	3575341	Fwd	EXM25_17815	*MAB_3593*	MgtC/SapB family protein	Y	Y

[1] Name given to strain arising from a GD01 Tn library colony that grew on a phage seeded plate
[2] The strain was isolated from a solid agar plate seeded with this phage; BPs, BPs*Δ33*HTH_HRM10
[3] Coordinate of the transposon insertion into strain GD01 (accession number CP035923.1)
[4] Direction of the hygromycin resistance gene open reading frame at the given coordinate
[5] The locus tag of the interrupted gene in strain GD01 (accession number CP035923.1) IR, Intergenic region
[6] The gene name of the *M. abscessus* ATCC 19977 homolog of the gene interrupted in *M. abs*cessus GD01. IR, Intergenic region
[7] Protein name or predicted function as determined by TPP synthesis pathway homologs or annotations of ATCC 19977 (NC_010397.1)
[8] The location of the transposon insertion was confirmed by a second PCR with primers designed to flank the insertion site. Y, Yes; ND, Not determined.
[9] The strain was streaked out to remove phage, grown in liquid media and tested for phage resistance by plaque assay. Y, Yes; ND, Not determined.
[10] In two instances, two strains isolated against the same phage were found to have identical transposon insertion sites

885 Table 2. Phage BPs and Muddy mutants escaping TPP-loss mediated resistance
886

Phage[1]	Parent[2]	Amino Acid Substitution[3]	Isolated on[4]	Reference
phKSW2	BPs∆*33*HTH_HRM10	gp22 L462R	*M. ab.* GD01Tn BPs_HRM10_RM6	This work
phKSW3	BPs∆*33*HTH_HRM10	gp22 A306V	*M. ab.* GD01Tn BPs_HRM10_RM6	This work
phKSW4	BPs∆*33*HTH_HRM10	gp22 L462R	*M. ab.* GD01Tn BPs_HRM10_RM11	This work
phKSW5	BPs∆*33*HTH_HRM10	gp22 A604E	*M. ab.* GD01Tn BPs_HRM10_RM11	This work
BPs_REM1	BPs∆*33*HTH_HRM10	gp22 L462R; G780R	*M. ab.* GD180_RM2	This work
phKSW1	BPs∆*33*HTH_HRM10	gp22 A604E	*M. smegmatis* ∆*MSMEG_5439*	This work
Muddy_REM1	Muddy	gp24 E680K	*M. ab.* GD180_RM2	This work
Muddy_HRM^{N0157}-1	Muddy	gp24 G487W	*M. tuberculosis* N0157	19
Muddy_HRM^{N0157}-2	Muddy	gp24 T608A	*M. tuberculosis* N0157	19
Muddy_HRM^{N0052}-1	Muddy	gp24 E680K	*M. tuberculosis* N0052	19

887
888 [1] Name of a phage able to form more clear plaques on TPP synthesis pathway mutants
889 [2] Parent phage from which the mutant was isolated
890 [3] Amino acid substitutions identified in mutant phages
891 [4] The *M. abscessus* or *M. tuberculosis* strain on which the mutant phage was isolated
892

893

894
895

896 Table 3. *M. abscessus* mutants spontaneously resistant to phage BPs derivatives
897

Resistant mutant[1]	Parent[2]	Isolated as resistant to[3]	Mutated gene[4]	Amino Acid Substitution[5]	Reference
GD17_RM1	*M. ab.* GD17	BPsHRM[GD03]	*pks*	G210V	[9]
GD22_RM4	*M. ab.* GD22	BPs∆*33*HTH_ HRM10 and Itos	*pks*	W2389fsX2406	[9]
GD38_RM2	*M. ab.* GD38	BPs∆*33*HTH_ HRM10	*pks*	M2115fsX2118	This work
GD59_RM1	*M. ab.* GD59	BPs∆*33*HTH_ HRM10 and Itos	*pks*	D327Y	This work
GD180_RM2	*M. ab.* GD180	BPs∆*33*HTH_ HRM10	*mmpL10*	S688fsX704	This work

898
899 [1] Resistant mutants were named after the parent strain and the number of the resistant mutant (RM) isolated
900 [2] Parent strain of *M. abscessus* from which the resistant mutant was isolated upon phage infection
901 [3] RMs were isolated by infecting cell cultures at a high MOI and plating infections on solid media to isolate
902 survivors
903 [4] The entire genomes of the resistant mutants were sequenced and compared to the genomes of the parents
904 to identify mutated genes conferring phage resistance
905 [5] The amino acid substitution in the protein product resulting from the gene mutation
906
907

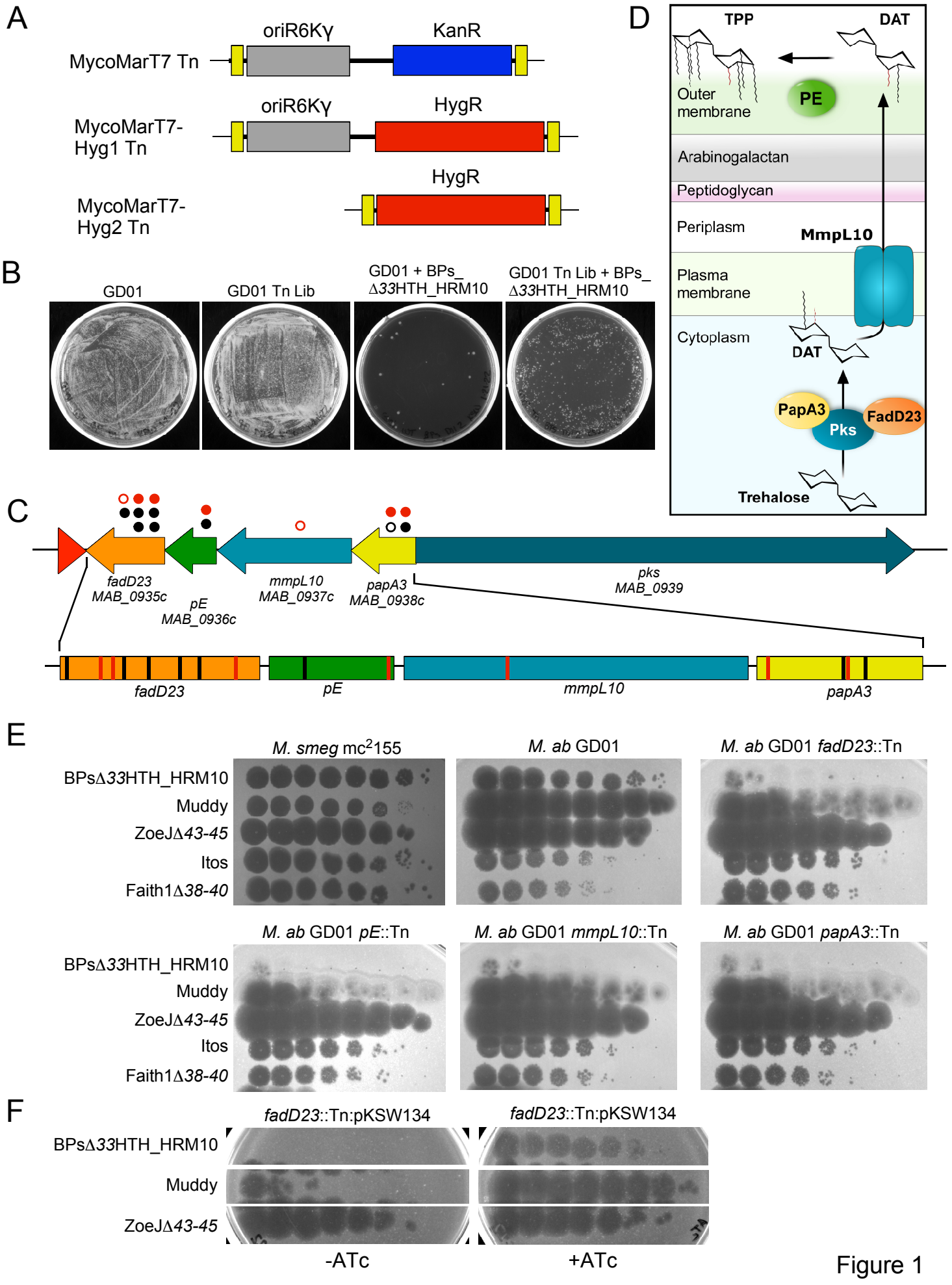
A
MycoMarT7 Tn
oriR6Kγ
KanR
MycoMarT7-Hyg1 Tn
oriR6Kγ
HygR
MycoMarT7-Hyg2 Tn
HygR
B
GD01
GD01 Tn Lib
GD01 + BPs_Δ33HTH_HRM10
GD01 Tn Lib + BPs_Δ33HTH_HRM10
C
fadD23 MAB_0935c
pE MAB_0936c
mmpL10 MAB_0937c
papA3 MAB_0938c
pks MAB_0939
fadD23
pE
mmpL10
papA3
D
TPP
DAT
Outer membrane
PE
Arabinogalactan
Peptidoglycan
Periplasm
MmpL10
Plasma membrane
Cytoplasm
DAT
PapA3
Pks
FadD23
Trehalose
E
M. smeg mc2155
M. ab GD01
M. ab GD01 fadD23::Tn
BPsΔ33HTH_HRM10
Muddy
ZoeJΔ43-45
Itos
Faith1Δ38-40
M. ab GD01 pE::Tn
M. ab GD01 mmpL10::Tn
M. ab GD01 papA3::Tn
BPsΔ33HTH_HRM10
Muddy
ZoeJΔ43-45
Itos
Faith1Δ38-40
F
fadD23::Tn:pKSW134
fadD23::Tn:pKSW134
BPsΔ33HTH_HRM10
Muddy
ZoeJΔ43-45
-ATc
+ATc

Figure 1

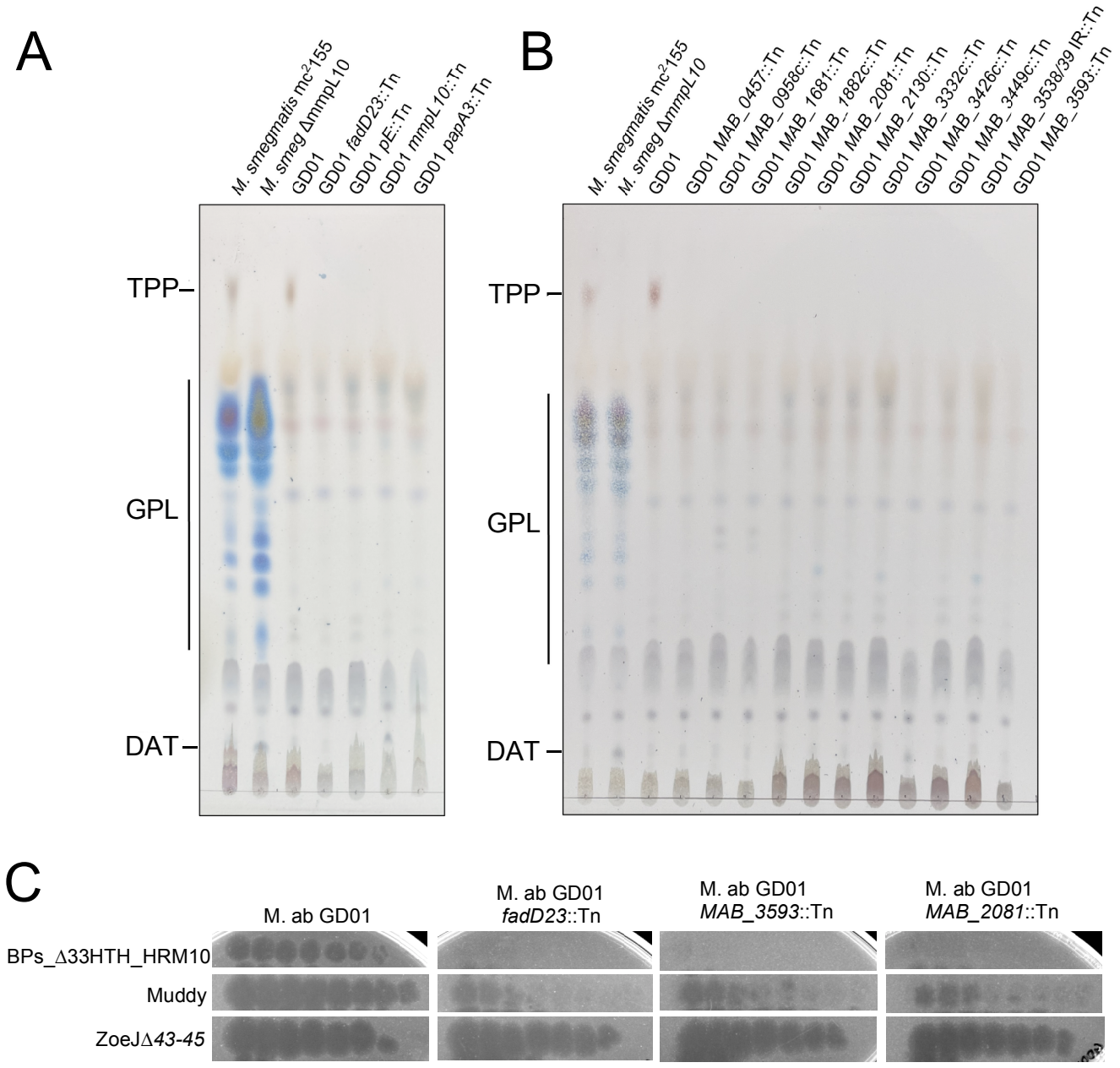
A
M. smegmatis mc²155
M. smeg ΔmmpL10
GD01
GD01 fadD23::Tn
GD01 pE::Tn
GD01 mmpL10::Tn
GD01 papA3::Tn
TPP
GPL
DAT
B
M. smegmatis mc²155
M. smeg ΔmmpL10
GD01
GD01 MAB_0457::Tn
GD01 MAB_0958c::Tn
GD01 MAB_1681::Tn
GD01 MAB_1882c::Tn
GD01 MAB_2081::Tn
GD01 MAB_2130::Tn
GD01 MAB_3332c::Tn
GD01 MAB_3426c::Tn
GD01 MAB_3449c::Tn
GD01 MAB_3538/39 IR::Tn
GD01 MAB_3593::Tn
TPP
GPL
DAT
C
M. ab GD01
M. ab GD01 fadD23::Tn
M. ab GD01 MAB_3593::Tn
M. ab GD01 MAB_2081::Tn
BPs_Δ33HTH_HRM10
Muddy
ZoeJΔ43-45

Figure 2

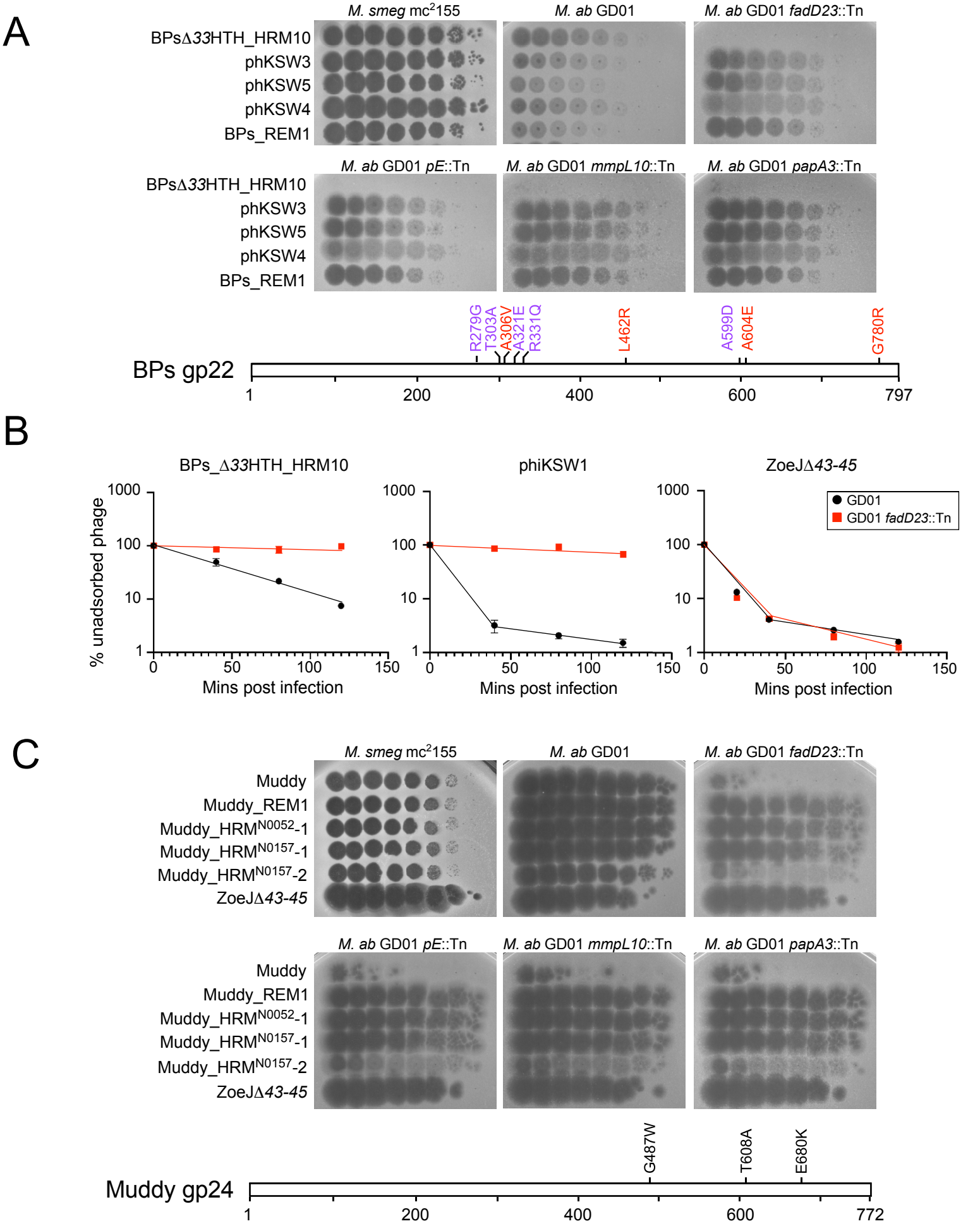
A
M. smeg mc²155
M. ab GD01
M. ab GD01 fadD23::Tn
BPsΔ33HTH_HRM10
phKSW3
phKSW5
phKSW4
BPs_REM1
M. ab GD01 pE::Tn
M. ab GD01 mmpL10::Tn
M. ab GD01 papA3::Tn
R279G
T303A
A306V
A321E
R331Q
L462R
A599D
A604E
G780R
BPs gp22
1
200
400
600
797
B
BPs_Δ33HTH_HRM10
phiKSW1
ZoeJΔ43-45
% unadsorbed phage
1000
100
10
1
0
50
100
150
Mins post infection
GD01
GD01 fadD23::Tn
C
Muddy
Muddy_REM1
Muddy_HRMN0052-1
Muddy_HRMN0157-1
Muddy_HRMN0157-2
ZoeJΔ43-45
G487W
T608A
E680K
Muddy gp24
1
200
400
600
772

Figure 3

A

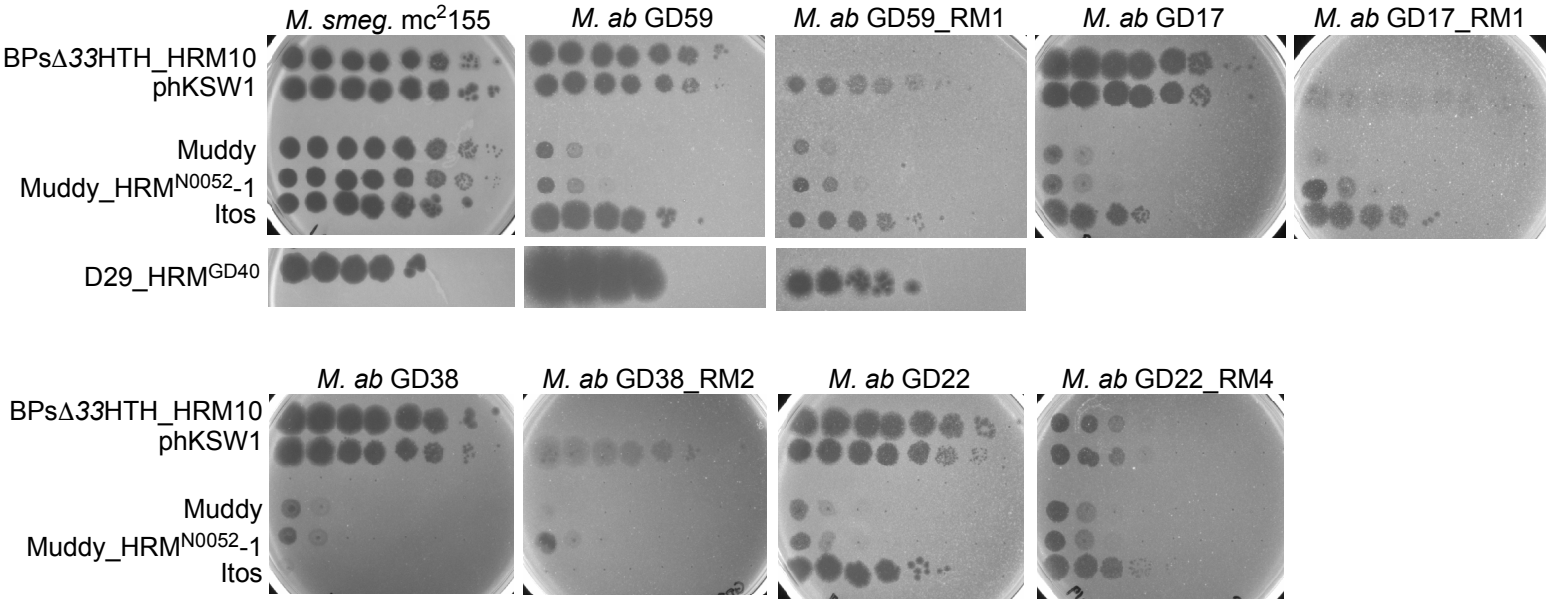
M. smeg. mc2155
M. ab GD59
M. ab GD59_RM1
M. ab GD17
M. ab GD17_RM1
BPsΔ33HTH_HRM10
phKSW1
Muddy
Muddy_HRMN0052-1
Itos
D29_HRMGD40
M. ab GD38
M. ab GD38_RM2
M. ab GD22
M. ab GD22_RM4
BPsΔ33HTH_HRM10
phKSW1
Muddy
Muddy_HRMN0052-1
Itos

B

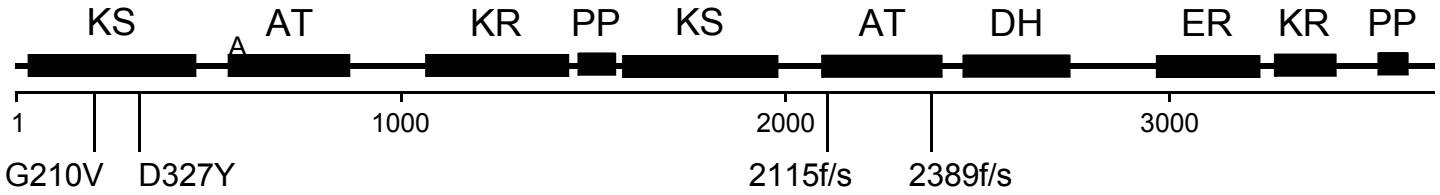
KS
AT
KR
PP
KS
AT
DH
ER
KR
PP
1
1000
2000
3000
G210V
D327Y
2115f/s
2389f/s

Figure 4

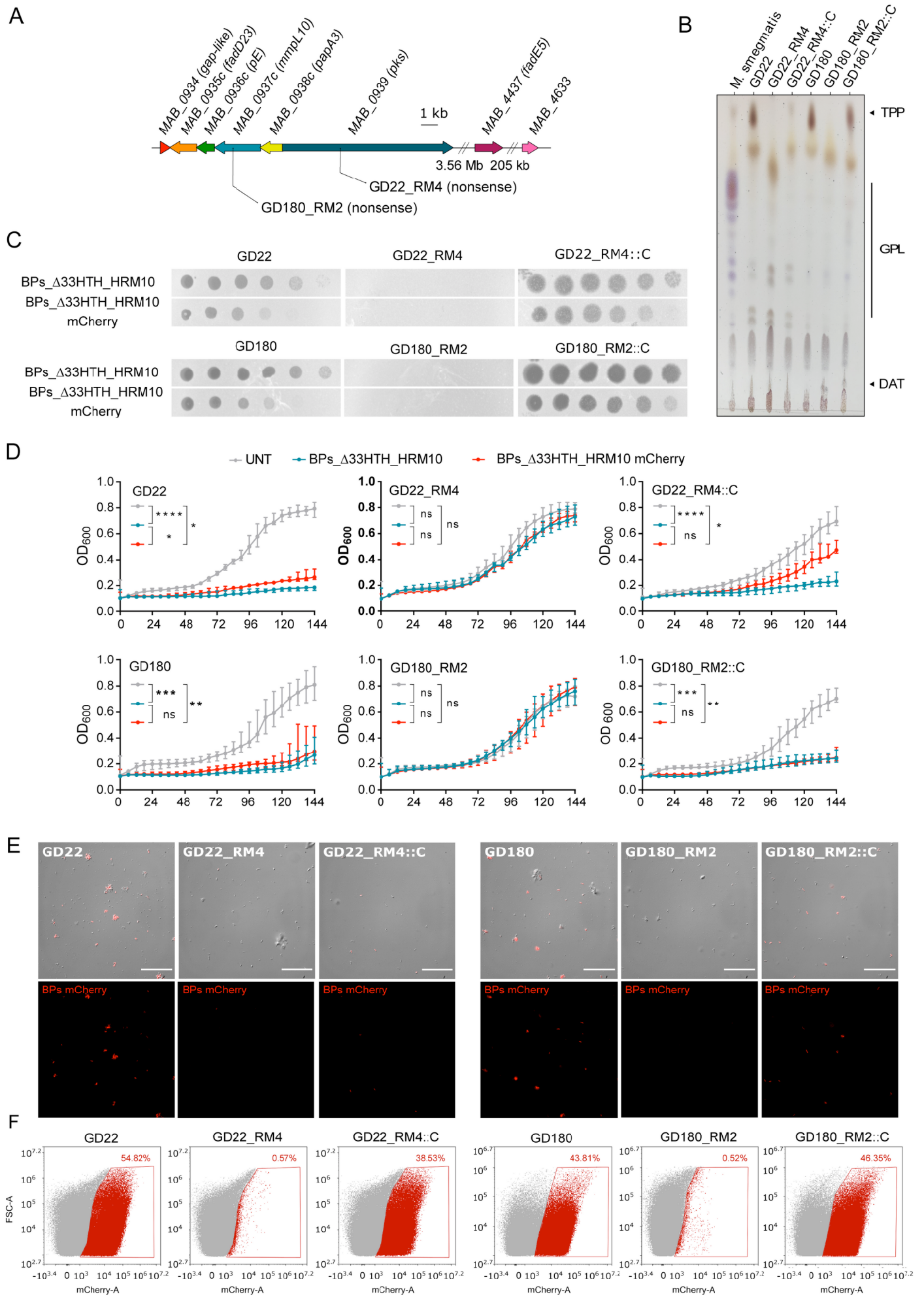
A
MAB_0934 (gap-like)
MAB_0935c (fadD23)
MAB_0936c (pE)
MAB_0937c (mmpL10)
MAB_0938c (papA3)
MAB_0939 (pks)
1 kb
MAB_4437 (fadE5)
MAB_4633
3.56 Mb 205 kb
GD22_RM4 (nonsense)
GD180_RM2 (nonsense)
B
M. smegmatis
GD22
GD22_RM4
GD22_RM4::C
GD180
GD180_RM2
GD180_RM2::C
TPP
GPL
DAT
C
GD22
GD22_RM4
GD22_RM4::C
BPs_Δ33HTH_HRM10
BPs_Δ33HTH_HRM10 mCherry
GD180
GD180_RM2
GD180_RM2::C
D
UNT
BPs_Δ33HTH_HRM10
BPs_Δ33HTH_HRM10 mCherry
OD600
E
GD22
GD22_RM4
GD22_RM4::C
GD180
GD180_RM2
GD180_RM2::C
BPs mCherry
F
FSC-A
mCherry-A
54.82%
0.57%
38.53%
43.81%
0.52%
46.35%

Figure 5

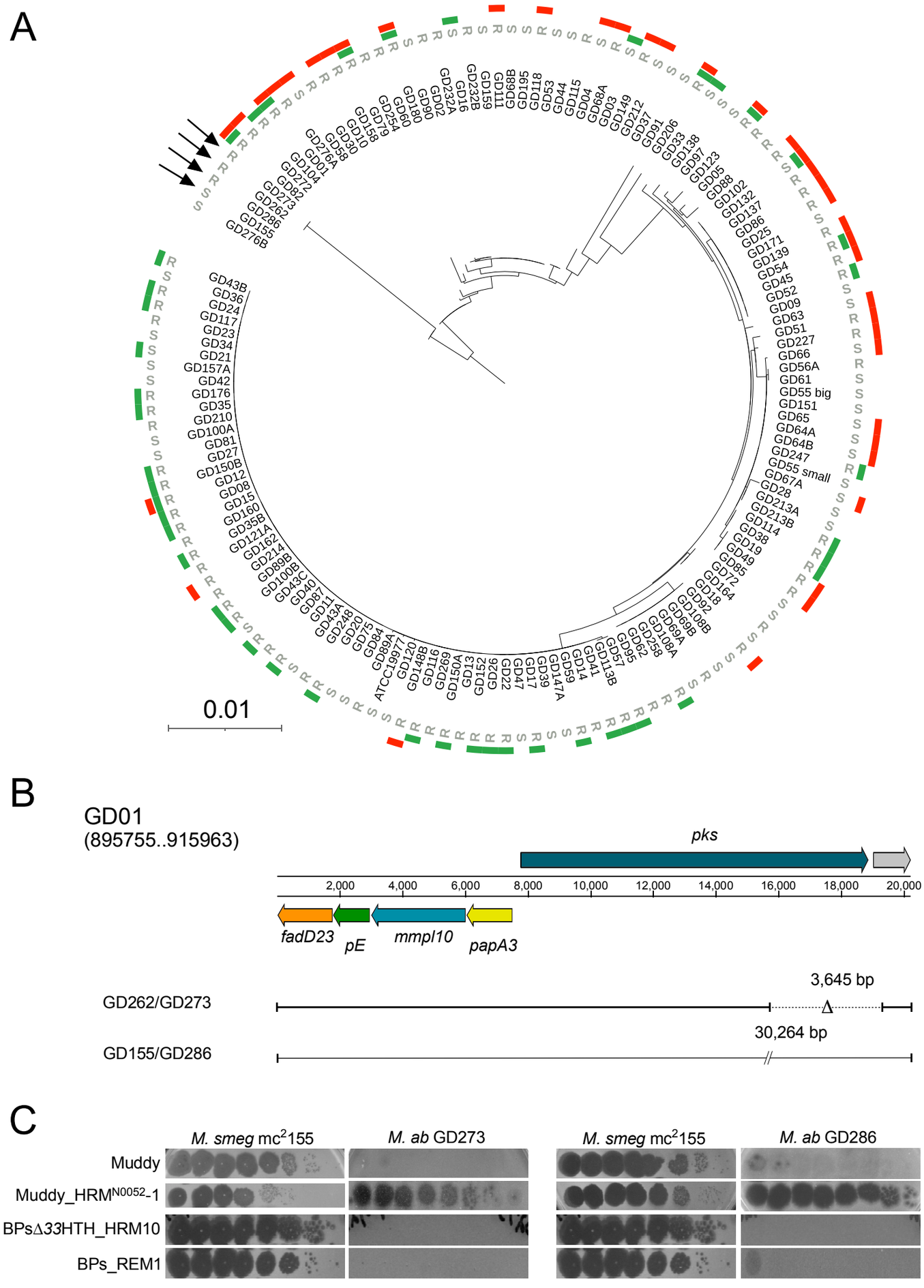
A
0.01
B
GD01
(895755..915963)
pks
2,000
4,000
6,000
8,000
10,000
12,000
14,000
16,000
18,000
20,000
fadD23
pE
mmpl10
papA3
3,645 bp
GD262/GD273
30,264 bp
GD155/GD286
C
M. smeg mc2155
M. ab GD273
M. smeg mc2155
M. ab GD286
Muddy
Muddy_HRMN0052-1
BPsΔ33HTH_HRM10
BPs_REM1

Figure 6

A

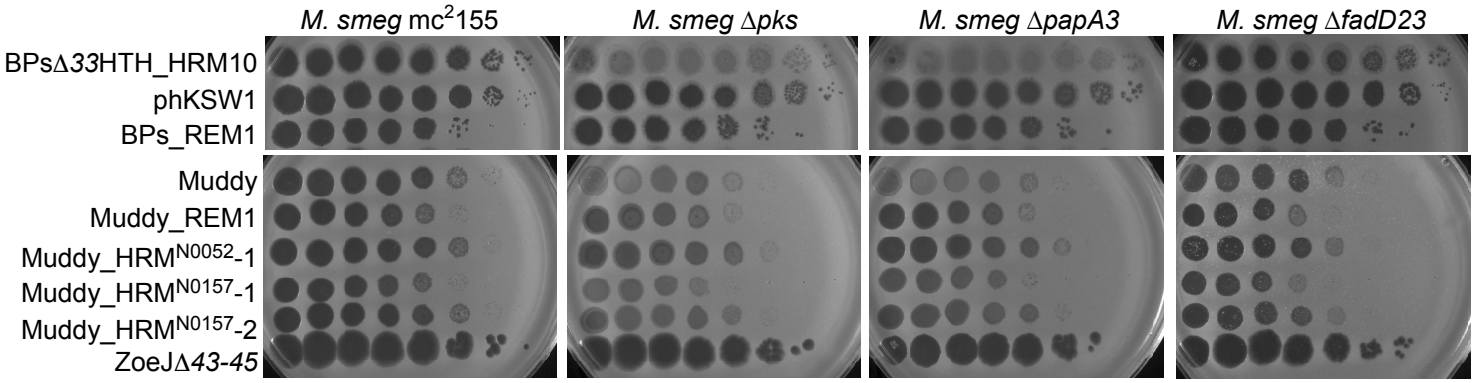

B

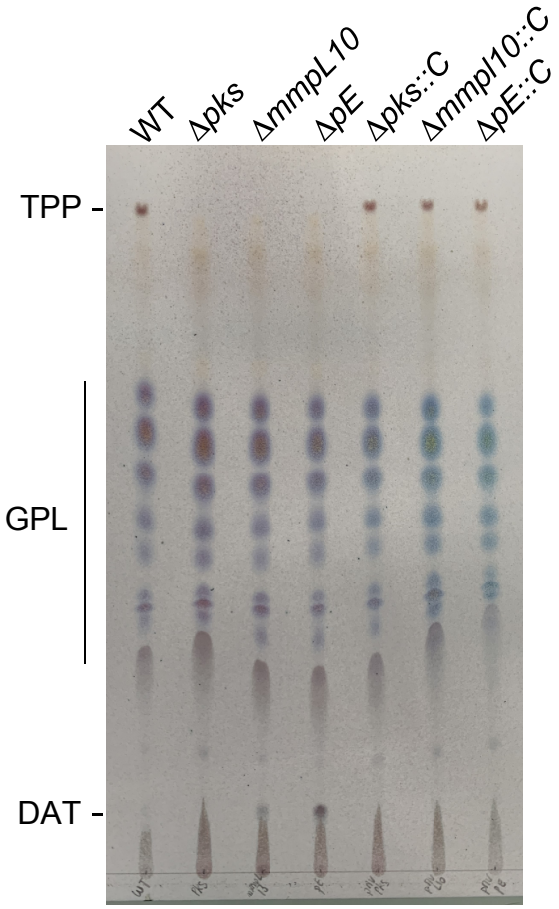

D

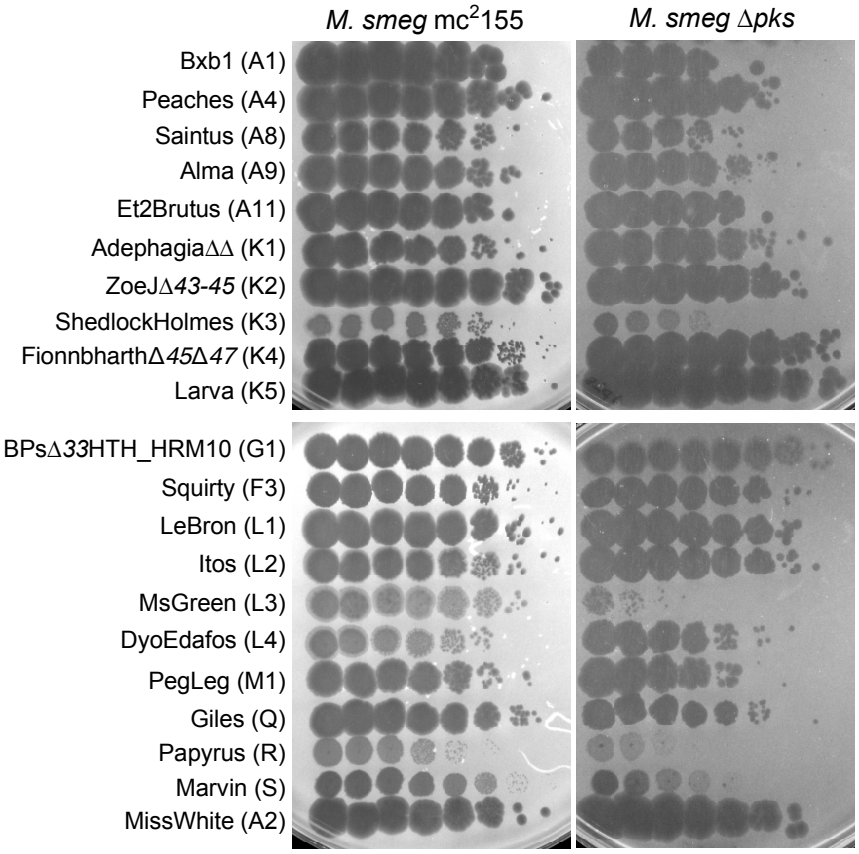

C

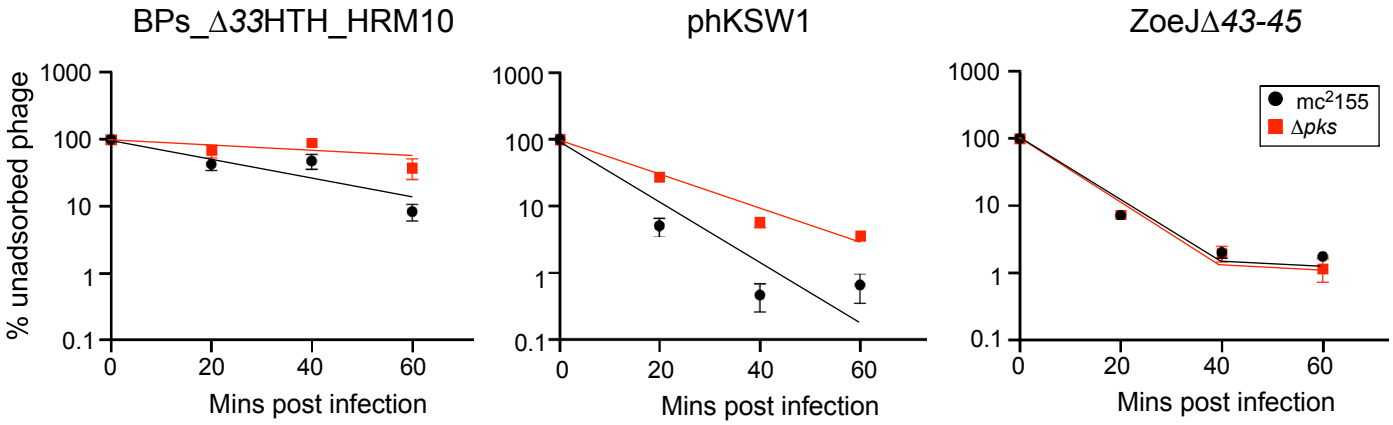

Figure 7